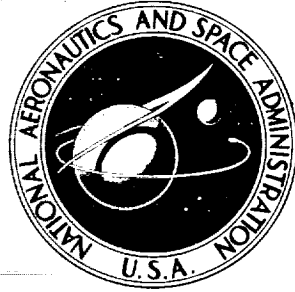


CASE FILE COPY

NASA TECHNICAL NOTE



NASA TN D-3081

NASA TN D-3081

A STUDY OF THE DYNAMICS OF AIRPLANE BRAKING SYSTEMS AS AFFECTED BY TIRE ELASTICITY AND BRAKE RESPONSE

by Sidney A. Batterson
Langley Research Center
Langley Station, Hampton, Va.

A STUDY OF THE DYNAMICS OF AIRPLANE BRAKING SYSTEMS
AS AFFECTED BY TIRE ELASTICITY AND BRAKE RESPONSE

By Sidney A. Batterson

Langley Research Center
Langley Station, Hampton, Va.

NATIONAL AERONAUTICS AND SPACE ADMINISTRATION

For sale by the Clearinghouse for Federal Scientific and Technical Information
Springfield, Virginia 22151 - Price \$3.00

A STUDY OF THE DYNAMICS OF AIRPLANE BRAKING SYSTEMS
AS AFFECTED BY TIRE ELASTICITY AND BRAKE RESPONSE

By Sidney A. Batterson
Langley Research Center

SUMMARY

An analog computer study of an automatic airplane braking system was made in which the effect of tire elasticity and the time required to apply and release brake torque were considered. The equations of motion were derived in general terms for a simplified single-wheel arrangement and then solved on the computer for the particular case of a wheel equipped with a 32×8.8 type VII tire. It was found that the braking-system efficiency depended on a complex interaction between the values of tire frequency, brake response time, and skid-control-sensor frequency, and depending on the combinations of these values, the braking-system efficiency could vary from 0 to 90 percent. The solutions also indicated that a braking system which operated satisfactorily in the presence of relatively high or medium coefficients of friction could operate unsatisfactorily at low coefficients of friction. It was also found that for low friction operation, large decreases in both stopping distance and tire skidding could be realized by proper selection of the wheel deceleration value used to generate the brake-release signal.

INTRODUCTION

The braking systems of most high-performance aircraft in use today utilize automatic anti-skid, or more appropriately, skid-control devices which regulate the torque applied by the brakes during the landing run. On dry and damp runways where the available coefficient of friction is large, the combined anti-skid control and brake system is efficient in minimizing airplane stopping distance and also is effective in preventing excessive tire skidding. On water- and slush-covered runways, however, where the available coefficient of friction can be small, a number of hazardous landing incidents have occurred which were attributed to inadequate braking. (See, for example, ref. 1.)

In an effort to obtain further insight into the phenomena which affect the basic operation of skid-control systems and also to determine the effect of low tire-ground friction coefficients on these systems during braking, an analog computer study was carried out for a simplified mathematical model of a braking system consisting of a skid control, brake, wheel, and tire. In this study, an effort was made to account for both the elastic behavior of the tire and the brake time response during cyclic braking.

With regard to the mechanical simulation programed for the computer, it should be pointed out that very little is known about the general dynamic behavior of a rolling wheel and elastic tire subjected to brake torque. This is particularly true of the mechanical properties of the tire and the forces that occur at the tire-ground interface. Therefore, it was not possible in this study to represent analytically some of the effects which are known to occur during braking; for example, the change in tire-rolling radius caused by stretching of the rubber, the variable location of the vertical center of ground pressure, and the development of ground force in the tire footprint area. Nevertheless, it is shown that the simulation chosen for this study resembles the observed dynamic behavior of actual wheels and tires subjected to braking forces.

The mathematical model of the braking system consisted of a rigid wheel and rigid tire connected by a spring and viscous damper to simulate the elastic and hysteresis properties of a pneumatic tire. The brake torque was programed to increase and decrease with time at various specified rates, and the signal to apply and release the brake torque was generated by a control that sensed wheel angular acceleration.

The basic dynamic equations for the braking system were derived in general terms and then solved on the analog computer for the specific case of a wheel and a 32 x 8.8 type VII tire having an initial horizontal velocity of 200 feet per second (60.96 m/s). The tire radius used in the computations was 1.16 feet (0.3536 m), and a constant vertical ground reaction of 22,000 pounds (97,856 N) was applied to the tire throughout the entire landing run. Solutions were made for a range of tire-runway friction coefficients, brake time responses, control frequencies, and acceleration values at which the control initiated the application and release of brake torque. The results indicated the effect of these parameters on stopping distance and tire skidding.

SYMBOLS

Measurements for this investigation were taken in the U.S. Customary System of Units. Equivalent values are indicated herein in the International System (SI) in the interest of promoting use of this system in future NASA reports. Details concerning the use of SI, together with physical constants and conversion factors, are given in reference 2.

C_{θ} torsional damping coefficient of wheel due to tire, $\frac{\text{lbf}}{\text{rad/sec}}$
 $\left(\frac{\text{N}}{\text{rad/sec}}\right)$

C_{ϕ} torsional damping coefficient of tire, $\frac{\text{lbf}}{\text{rad/sec}}$ $\left(\frac{\text{N}}{\text{rad/sec}}\right)$

C_{β} torsional damping coefficient of control sensor, $\frac{\text{lbf}}{\text{rad/sec}}$ $\left(\frac{\text{N}}{\text{rad/sec}}\right)$

$C_{C,\theta}$	critical torsional damping coefficient of wheel, $\frac{\text{lbf}}{\text{rad/sec}} \left(\frac{\text{N}}{\text{rad/sec}} \right)$
$C_{C,\phi}$	critical torsional damping coefficient of tire, $\frac{\text{lbf}}{\text{rad/sec}} \left(\frac{\text{N}}{\text{rad/sec}} \right)$
$C_{C,\beta}$	critical torsional damping coefficient of control sensor, $\frac{\text{lbf}}{\text{rad/sec}} \left(\frac{\text{N}}{\text{rad/sec}} \right)$
D	drag load between tire and ground, lbf (N)
g	acceleration due to gravity, ft/sec ² (m/sec ²)
I_W	moment of inertia of wheel, ft-lbf-sec ² (kg-m ²)
I_T	moment of inertia of tire, ft-lbf-sec ² (kg-m ²)
I_β	moment of inertia of control sensor, ft-lbf-sec ² (kg-m ²)
k_T	spring constant of tire, lbf/ft (N/m)
k_β	spring constant of control sensor, lbf/ft (N/m)
n	control sensor mass radius, ft (m)
Q_i	generalized force where $i = x, \theta, \phi,$ and β
q_i	generalized coordinate where $i = x, \theta, \phi,$ and β
r_W	wheel radius, ft (m)
r_T	tire radius, ft (m)
r_e	effective tire-rolling radius during braking, ft (m)
$r_{e,0}$	effective tire-rolling radius during free rolling, ft (m)
S_W	slip ratio of wheel
S_T	slip ratio of tire
T	total kinetic energy of braking system, ft-lbf (m-N)
T_B	braking torque, ft-lbf (m-N)

$T_{B,L}$	braking torque during wheel locked condition, ft-lbf (m-N)
$T_{B,max}$	maximum braking torque, ft-lbf (m-N)
t	time, sec
t_1	time for brake torque to increase from zero to its maximum, sec
t_2	time for brake torque to decrease from its maximum value to zero, sec
V	potential energy, ft-lbf (m-N)
V_T	potential energy of tire due to elastic deformation of tire, ft-lbf (m-N)
V_β	potential energy of sensor mass due to elastic deformation of sensor spring, ft-lbf (m-N)
W	total weight, lbf (N)
W_{skid}	work done by tire in skidding, ft-lbf (m-N)
x	linear displacement of wheel axle, ft (m)
\dot{x}_0	initial forward velocity, ft/sec (m/sec)
y_T	tire circular spring deflection, ft (m)
y_β	control sensor circular spring deflection, ft (m)
β	angular displacement of control sensor mass, rad
$\ddot{\beta}_1$	control sensor acceleration value that generates brake application signal, rad/sec ²
$\ddot{\beta}_2$	control sensor acceleration value that generates brake release signal, rad/sec ²
η	braking-system efficiency, $\frac{\text{Minimum stopping distance}}{\text{Actual stopping distance}} \times 100$, percent
θ	angular displacement of wheel, rad
μ	coefficient of friction
μ_{max}	maximum obtainable coefficient of friction between tire and ground
μ_{skid}	coefficient of friction at zero tire angular velocity

ξ_θ	torsional damping ratio of wheel due to tire
ξ_φ	torsional damping ratio of tire
ξ_β	torsional damping ratio of control sensor
σ	skid index, $\frac{\text{Total work done by tire in skidding}}{\text{Initial airplane kinetic energy}} \times 100$, percent
φ	angular displacement of tire, rad
$\omega_{n,\theta}$	natural frequency of wheel on tire, rad/sec
$\omega_{n,\varphi}$	natural frequency of tire on wheel, rad/sec
$\omega_{n,\beta}$	natural frequency of sensor mass, rad/sec

Dots over symbols indicate differentiation with respect to time.

MATHEMATICAL MODEL AND METHOD OF ANALYSIS

The physical system programed for the analog computer is shown schematically in figure 1. It consists of a rolling wheel and tire with the total mass concentrated at the axle and is traveling in the x-direction. The wheel is rigid and for the purpose of this analysis the tire is also assumed to be rigid and is connected to the wheel by a linear spring and dashpot in order to represent the elastic and damping characteristics of the tire. The wheel is subjected to a braking torque T_B which causes relative motion between the wheel and tire. The resulting spring, damping, and tire inertia forces produced by this motion causes a drag force D to act between the tire and the ground. This drag force is expressed as $D = \mu W$ where μ is the coefficient of friction between the tire and the ground, and W is the total weight. The angular displacement of the wheel is designated θ and the angular displacement of the tire is designated φ . The skid-control-sensor unit

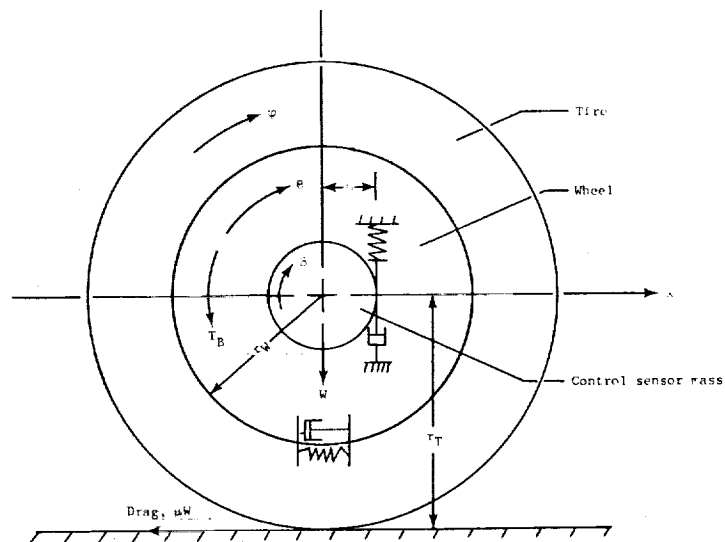


Figure 1.- Mathematical model of braking system.

is simulated by a balanced cylindrical mass free to pivot about the axle center line and is restrained by a spring and dashpot attached to the wheel as shown schematically in figure 1. The angular displacement of the sensor mass is designated β . The computer was programed to generate brake application and brake release signals at certain preselected values of β (the angular acceleration of the sensor mass).

Although current skid-control systems are much more sophisticated than this acceleration type, it was selected on the basis of simplicity for this first analysis. The operation of this type of control unit is identical to the operation of many standard angular accelerometer instruments and some of the first on-off skid-control units operated in this manner. It is assumed that throughout the braking run, the vertical ground reaction is directly beneath the wheel center and remains equal to the total weight.

Equations of Motion

The variables x , θ , φ , and β are considered as generalized coordinates, and it is shown in appendix A that the equations of motion of the system are

$$\ddot{x} = -\mu g \quad (1)$$

$$\ddot{\theta} - 2\omega_{n,\theta}\xi_{\theta}(\dot{\varphi} - \dot{\theta}) - \omega_{n,\theta}^2(\varphi - \theta) = \frac{T_B}{I_W} \quad (2)$$

$$\ddot{\varphi} + 2\omega_{n,\varphi}\xi_{\varphi}(\dot{\varphi} - \dot{\theta}) + \omega_{n,\varphi}^2(\varphi - \theta) = \frac{\mu W r_T}{I_T} \quad (3)$$

$$\ddot{\beta} = -2\omega_{n,\beta}\xi_{\beta}(\dot{\beta} - \dot{\theta}) - \omega_{n,\beta}^2(\beta - \theta) \quad (4)$$

In order to obtain a solution for these equations, it is necessary to define a set of initial conditions and also to define a variation for μ and T_B in terms of known quantities. The initial conditions are obtained by selecting an initial forward speed \dot{x}_0 which then defines the initial values of $\dot{\theta}$, $\dot{\varphi}$, and $\dot{\beta}$ through the kinematic relation for free rolling. The initial displacements x , θ , φ , and β are taken equal to zero.

Coefficient of Friction

The variation of the coefficient of friction is defined in a somewhat different manner than is followed in current practice. As pointed out previously, the wheel and the tire can have different motions because the tire is considered to deform elastically under the application of brake torque (simulated in this

case by the spring connecting the tire and wheel), whereas the wheel is assumed to be rigid. It is clear that since the coefficient of friction is a function of the relative motion between two rubbing surfaces, the coefficient of friction between the tire and runway must be a function of the tire motion $\dot{\varphi}$ with respect to the runway rather than of the wheel motion $\dot{\theta}$. It is customary in current practice to define the variation of the coefficient of friction μ as a function of the slip ratio, where the slip ratio is defined as

$$S_W = 1 - \frac{\dot{\theta}}{\dot{x}/r_e} \quad (5)$$

where S_W is the slip ratio defined as a function of wheel angular velocity, $\dot{\theta}$ is the wheel angular velocity, \dot{x} is the axle linear velocity, and r_e is the tire-rolling radius.

The wheel angular velocity is used in equation (5) since in experimental testing this quantity can be easily measured during the application of brake torque, whereas the velocity of the tire in the footprint would be very difficult to obtain. The equations of motion (eqs. (1) to (4)), however, provide a solution for the tire velocity $\dot{\varphi}$; therefore, in this analysis the slip ratio between the tire and the ground is used and is defined in a somewhat similar manner as

$$S_T = 1 - \frac{\dot{\varphi}}{\dot{x}/r_T} \quad (6)$$

where S_T is the slip ratio defined as a function of tire angular velocity, $\dot{\varphi}$ is the tire angular velocity, and r_T is the tire radius. (See fig. 1.)

In order to define the relation between μ and S_T , it was assumed that as torque was applied to the freely rolling wheel, no slip occurred between the tire and runway surface until the maximum apparent coefficient of friction was developed. The maximum apparent coefficient is defined as the maximum coefficient of friction that could be developed at the tire-ground interface at the instant under consideration. This maximum coefficient is indicated symbolically as μ_{\max} . The assumption of no slip (that is, $S_T = 0$) from free rolling until the instant when μ_{\max} is reached presupposes that the coefficient developed within this range depends primarily on tire stiffness, and this supposition is in general agreement with the opinions expressed by a number of investigators. (See refs. 3, 4, and 5.) Some experimental results, which also tend to bear out this simulation, will be discussed subsequently.

If the brake torque is increased following the attainment of μ_{\max} , the tire starts slipping with respect to the ground and the slip ratio S_T takes on increasing values. A value of S_T of 1 indicates that the tire is in a full skid and has no rotational motion; that is, $\dot{\varphi} = 0$. The coefficient of friction

associated with a full skid is indicated symbolically as μ_{skid} . In general, for the conditions of interest in the stopping of airplanes, μ_{max} can be considered greater than μ_{skid} .

The manner in which the coefficient of friction varies with slip ratio for coefficients lying in the region between μ_{max} and μ_{skid} depends on a large number of variables which include, for example, surface roughness, tire tread, tire and ground temperature, runway contamination, tire pressure, and so forth. Because little is known of the manner in which the coefficient varies with many of these parameters, and because some vary in a random manner throughout a braking stop, an empirical relation was formulated for use in the analog-computer study. To obtain this relation, use was made of experimental braking data obtained during the tests reported in reference 6. The data were normalized by using the ratio of instantaneous friction coefficient to maximum coefficient μ/μ_{max} . The experimental data points which were obtained during the first braking cycle of some of the dry surface runs are plotted in figure 2. As would be expected, these data scatter over a wide band because, as pointed

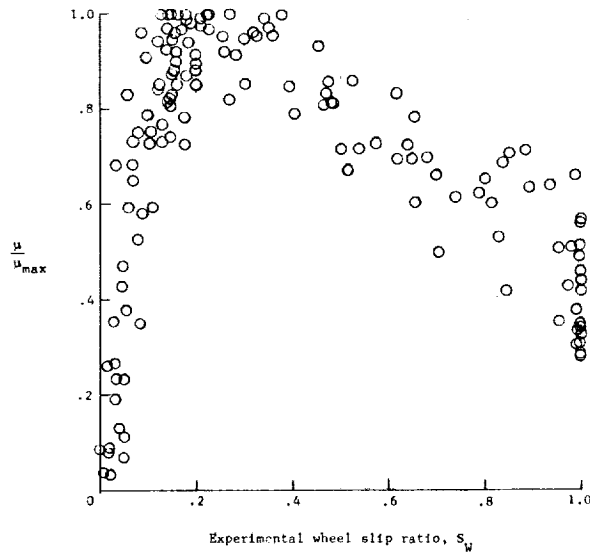


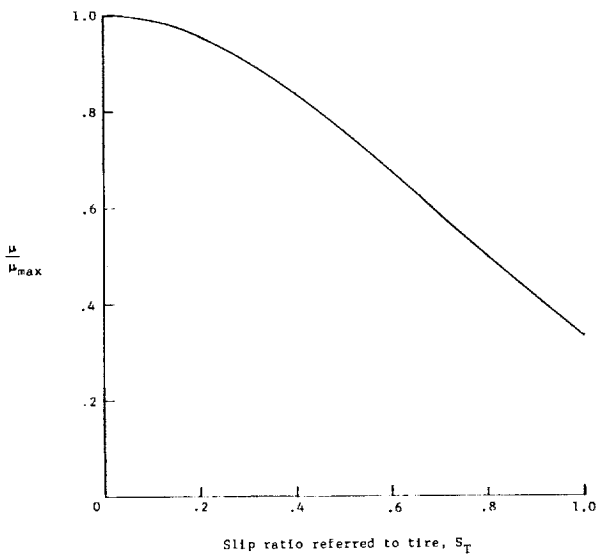
Figure 2.- Variation of friction coefficient with wheel slip ratio obtained from experimental braking test on a dry concrete surface with a 32 x 8.8 type VII tire. (Data obtained from ref. 6.)

out previously, the value of the coefficient depends on a number of variables, some of which vary in an unpredictable manner. For this reason there is no unique curve from a practical standpoint that describes the variation of μ with S_T for values of $S_T > 0$. The variation for $S_T > 0$ chosen for the analog computations was, therefore, obtained by choosing an expression which gave an average fairing of the experimental data.

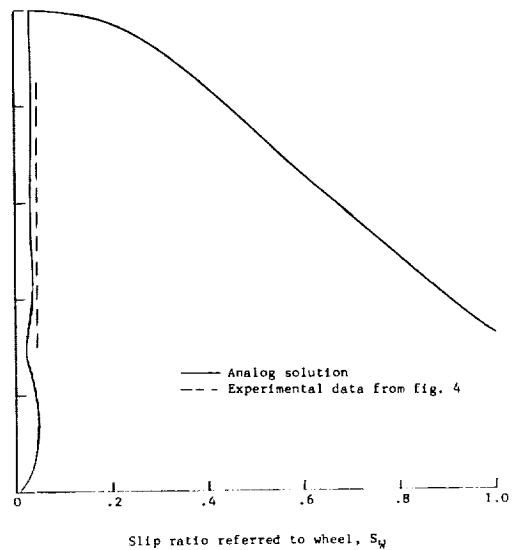
The variation of μ/μ_{max} with S_T used in the calculations is shown in figure 3(a). Since S_T is the slip ratio referred to the tire, and since it was assumed that no slip occurred in the tire footprint until μ reached the value of μ_{max} , it can be seen that the slip S_T is equal to zero in this region (from free rolling where $\mu = 0$ until $\mu = \mu_{max}$). The empirical expression used to define the variation to the right of where μ_{max}

occurs (sometimes referred to as the back side of the μ -slip curve for the tire) that is, for values of $S_T > 0$ is

$$\frac{\mu}{\mu_{max}} = \left(\frac{1}{3}\right) S_T^2 \quad (7)$$



(a) Analog simulation of variation of friction coefficient with tire slip ratio.



(b) Variation of friction coefficient with wheel slip ratio.

Figure 3.- Experimental braking data and analog outputs of the variation of friction coefficient with tire and wheel slip ratios for an initial braking cycle.

For values of $S_T > 1$ the value of the coefficient of friction was taken equal to that for $S_T = 1$.

Figure 3(b) is an actual curve obtained from the analog computer of a first-cycle braking variation using the simulation shown in figure 1. In figure 3(b) μ/μ_{max} is plotted against S_W , the slip ratio referred to the wheel, which is the manner in which data on the variation of μ with slip ratio are commonly presented. It can be seen that this initial braking cycle has, in general, the form of curves usually obtained from experimental braking tests; that is, μ_{max} occurs at a slip ratio greater than zero and the values of S_W to the left of the peak (sometimes referred to as the front side of the μ -slip curve for the wheel) depend primarily on the tire stiffness.

To justify further the simulation of μ with S_T used for this analog study in the region between $\mu = 0$ and $\mu = \mu_{max}$, some data from the experimental braking tests reported in reference 6 are presented in figure 4. The curve associated with the square symbols was obtained during a free-rolling test at a forward speed of about 150 ft/sec (45.72 m/sec); that is, no braking torque was applied to the wheel. The other curve was obtained for a test made at the same forward speed by using the same 32×8.8 type VII tire; however, during this test, brake torque was being applied to the wheel and was increasing approximately linearly with time throughout the distance indicated by the data. At the start of the measurements, the brake-torque value was about one-quarter of that required for locking the wheel, whereas at the time that the last data point was obtained, the brake torque was approaching the value necessary to develop μ_{max} . The instrumentation used for these tests provided for extreme accuracy in measuring and correlating the parameters of distance traveled x and wheel angular displacement θ . The static vertical

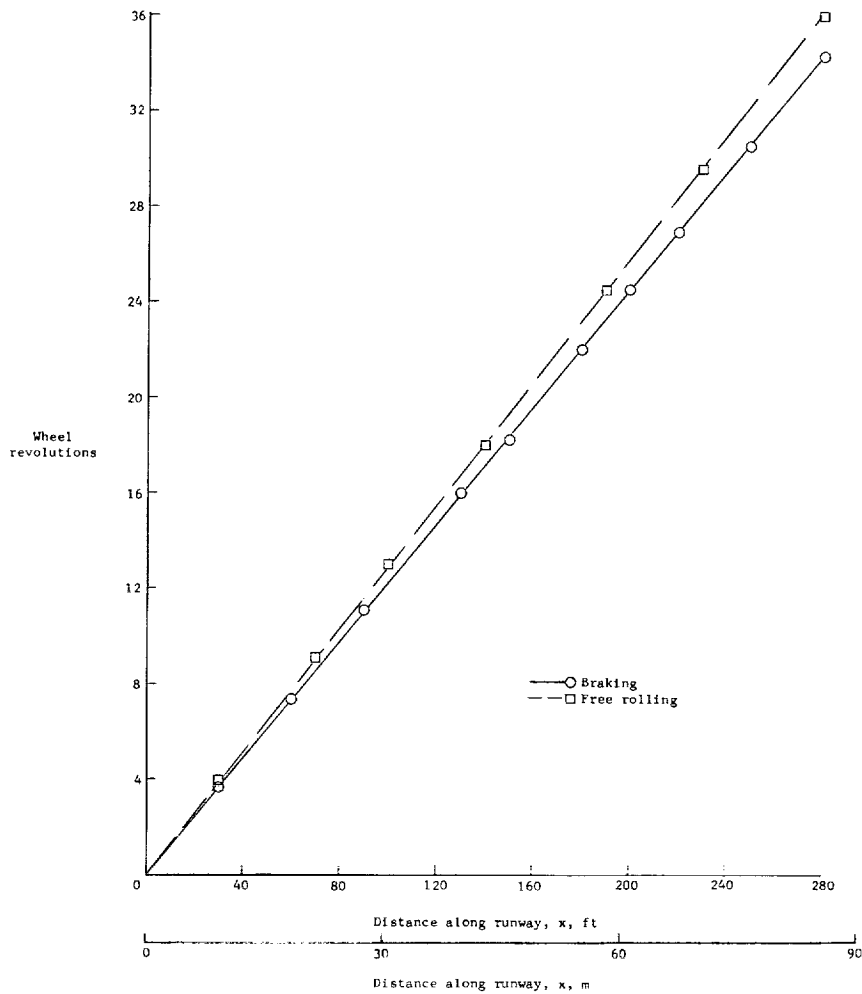


Figure 4.- Experimental variation of wheel rotation with distance traveled obtained during a braking test and a free-rolling test made with a 32 x 8.8 type VII tire. Static load on tire, 10,000 lb (44,800 N); horizontal velocity, 150 ft/sec (45.72 m/sec). (Data obtained from tests of ref. 6.)

load for both tests was 10,000 pounds (44,480 N) and the tire pressure was 260 pounds per square inch (179.26 N/cm²). It can be seen that the value of S_W , despite the increasing brake torque, is apparently constant since the curves are straight lines and have a common origin. The value of S_W for the braking run can be computed from the equation given in reference 7 as

$$S_W = \frac{r_e - r_{e,0}}{r_e}$$

where r_e is the effective tire-rolling radius during braking, and $r_{e,0}$ is the effective tire-rolling radius during free rolling.

The data presented in figure 4 yield values of r_e of 1.31 ft (0.3993 m) and $r_{e,0}$ of 1.25 ft (0.3810 m); therefore, $S_W = 0.046$.

In figure 3(b) the computed value of S_W was also approximately constant for the upper 75 percent of the front side of the curve of variation of μ with S_W (hereafter designated μ -slip curve for the wheel). Also the computed value for S_W in figure 3(b) is seen to average slightly over 0.03. The dotted line in figure 3(b) is the experimental braking data of figure 4. This excellent agreement between the experimental braking results, and the results obtained from the analog computer would indicate that the variation of μ with S_T chosen herein (fig. 3(a)) to simulate the action of an elastic tire during the application of brake torque gives a very good description of the actual variation.

In order to use the variation of μ with S_T shown in figure 3(a), it was necessary to program the computer to calculate μ by two different methods. The particular method used at the instant the calculation was being made depended on whether S_T was equal to zero or greater than zero. During the time $S_T = 0$, the variable ϕ and its time derivatives were eliminated from equations (2) and (3) by using the expression

$$\phi = \frac{x}{r_T}$$

which expresses the kinematic relation between the variables ϕ and x when the tire is rolling without slipping, that is, $S_T = 0$. During this time, the computer operated in a mode which calculated the variables μ , x , θ , and β , and μ for this case was a function of tire elasticity, damping, and inertia. While in this mode of operation, the computer was programed to compare the value calculated for μ with the value of μ_{max} given for the particular run. When the calculated value of μ became greater than μ_{max} , the computer switched over to a second mode of operation. In this second mode, the computer calculated the value of μ as given by equation (7) and also calculated the values of x , θ , ϕ , and β by using equations (1) to (4). While in this mode of operation, the computer was programed to examine the value of S_T and continued to operate in this mode as long as S_T was greater than zero. When S_T became zero, the computer switched back to the first mode of operation. The computer then operated throughout the entire run and switched modes according to this described logic system. It should be pointed out that the value of μ calculated in the first mode is not in a true sense a coefficient of friction since it does vary and no sliding occurs. It can, however, be interpreted as an apparent coefficient of friction.

Brake Torque

In this study, the brake was considered to be torque limited and the limiting value is indicated as $T_{B,max}$, and it was further assumed that when brake

torque was applied or released, it varied linearly with time. Although the linear variation is never obtained in practice, the actual variation between brakes and brake installations can vary so widely that this linear variation was chosen in the interests of simplicity for this first analysis. The brake-torque-time variation used is illustrated schematically by the solid line in figure 5. The time for torque to increase from 0 to its limited value $T_{B,max}$ is called t_1 and the time to decrease from $T_{B,max}$ to 0 is called t_2 . Values of t_1 and t_2 could be selected at will in order to simulate brakes having various response times.

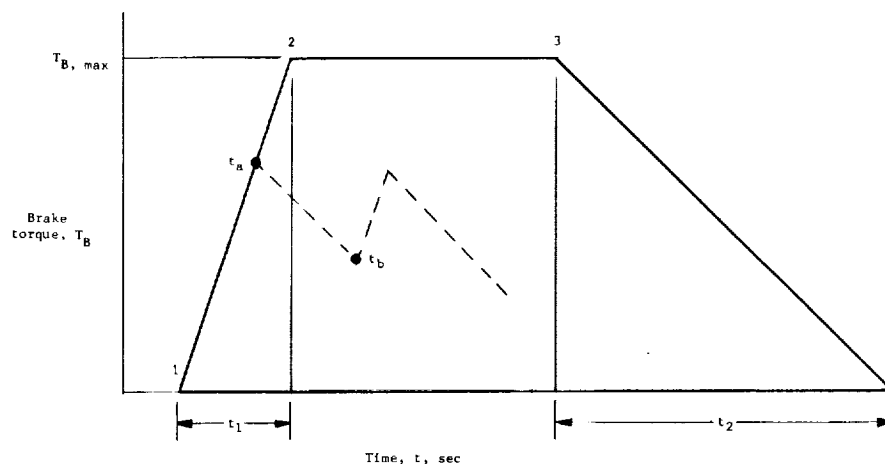


Figure 5.- Variation of brake torque with time used in analog computer braking study.

The computer was programed to permit the brakes to be released prior to reaching $T_{B,max}$ or they could be reapplied during the release interval before reaching zero torque. For example, refer to figure 5 and suppose that the brake torque is increasing and at time t_a a release signal is generated by the accelerometer; at that instant the brake torque will start decreasing at a rate equal to that indicated by line 3-4. Of course, if the release signal occurred some time after point 2 on line 1-2 was reached, the brake torque would continue at this constant limiting value from the point 2 until the release signal was generated. If a brake application signal is generated before the torque reaches zero, for example, at time t_b , the torque will start increasing at a rate equal to that indicated by line 1-2. This cycling process is repeated by the computer throughout the entire landing runout, the brake torque being subject to the command signals generated by the control.

Wheel Locking

In many instances during the computer runs, the dynamic conditions of the problem were such as to allow the wheel to lock during certain portions of the runout; that is, the response of the brakes and/or the control was not fast enough in reducing brake torque to prevent the wheel from being braked to a complete stop. In order to eliminate prolonged periods of wheel locking, the

computer was programed to generate a brake release signal when the wheel angular velocity was less than 10 radians per second. Even so, some wheel locking did occur, and during this time the brake torque applied to the wheel was a function of the tire inertia and the applied ground drag torque. The locked-wheel brake torque $T_{B,L}$ is shown in appendix B to be

$$T_{B,L} = I_T \ddot{\phi} - \mu W r_T \quad (8)$$

When wheel locking occurred, the computer was programed to compute both T_B and $T_{B,L}$ and to compare the two values. As long as T_B was greater than $T_{B,L}$, the wheel remained locked and the brake torque used in the equations was $T_{B,L}$. When, however, T_B became less than $T_{B,L}$, the value of T_B was used in the equations and the wheel began turning once again. During wheel-locked conditions, $T_{B,L}$ appears as an oscillation in brake torque at the tire frequency because of the oscillatory nature of $\ddot{\phi}$ immediately following wheel locking. (See fig. 6.)

Tire Skidding

An important factor used for judging the performance of a braking system is the amount of tire skidding that occurs during the braking run. Tire wear, particularly at the higher coefficients of friction, depends largely on the amount of work done in skidding. Also, the amount of cornering force that can be developed is affected by tire skidding. The total work done in skidding is shown in appendix C to be:

$$W_{skid} = W \int_{t=0}^{t=t} \mu S_T \dot{x} dt \quad (9)$$

where

W_{skid} work done in skidding

W vertical wheel load

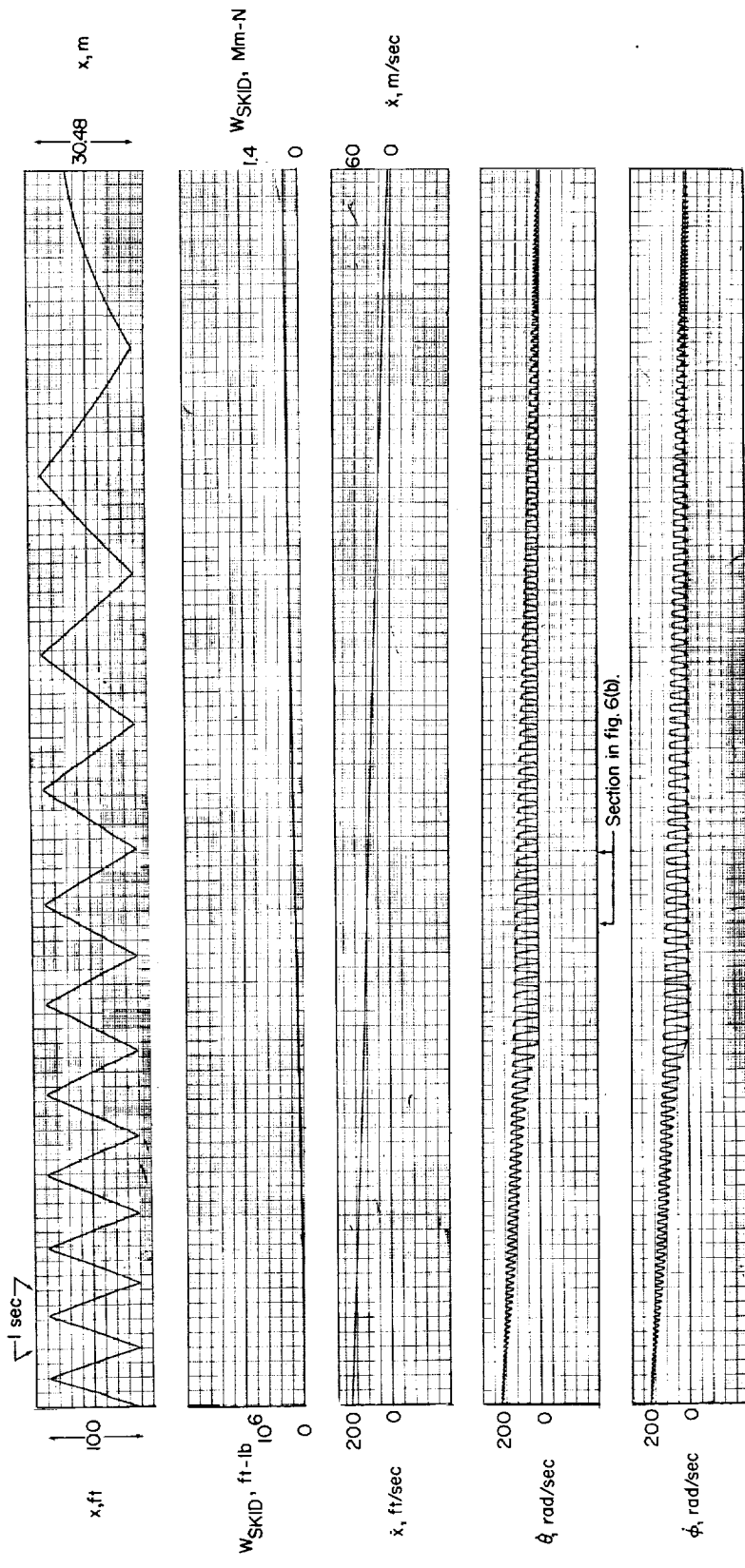
μ instantaneous coefficient of friction

S_T instantaneous slip ratio referred to tire

\dot{x} instantaneous forward speed

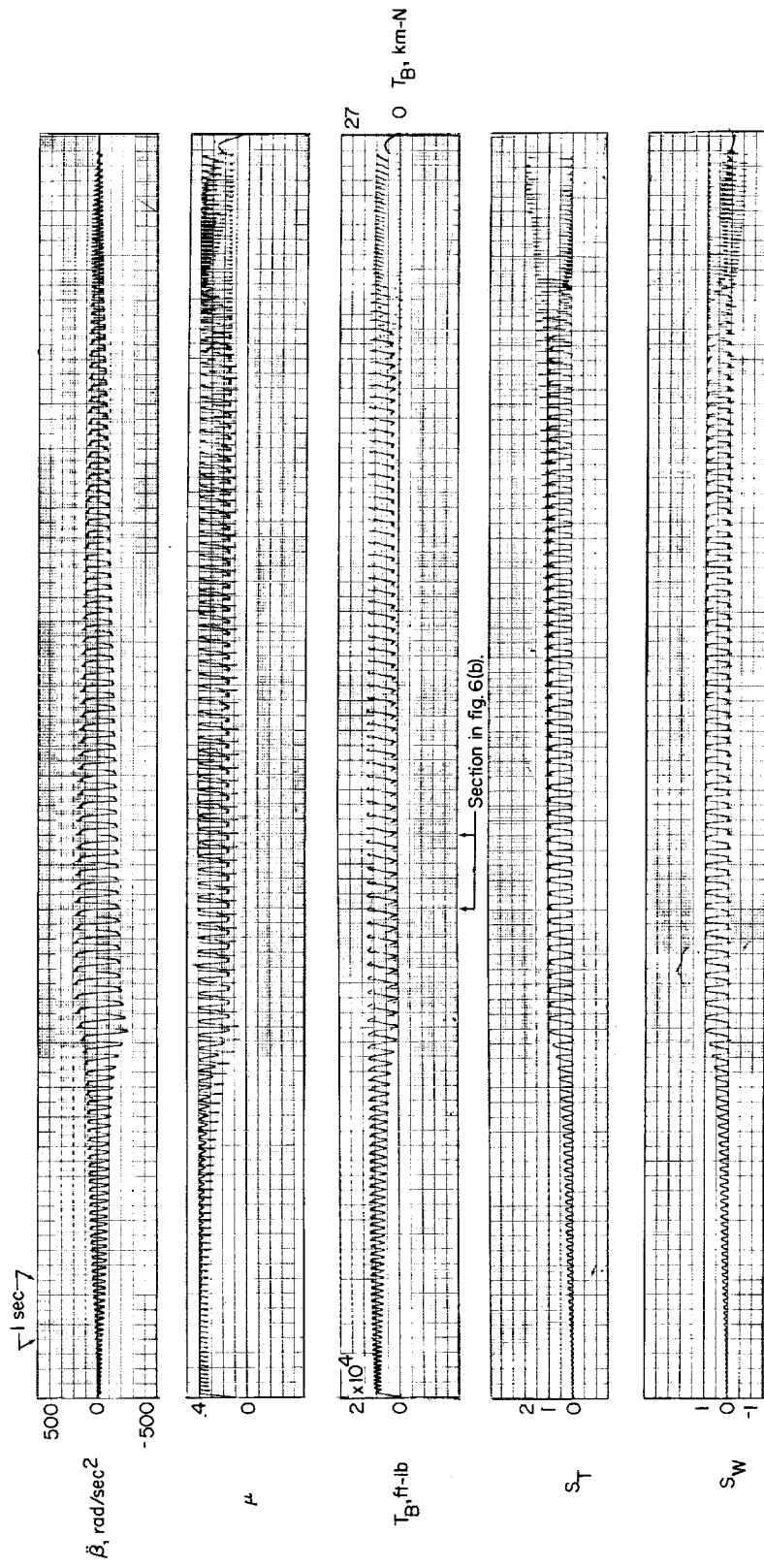
t time

The analog computer was programed to solve equation (9) and produced a time history of the work done in skidding throughout the entire braking stop.



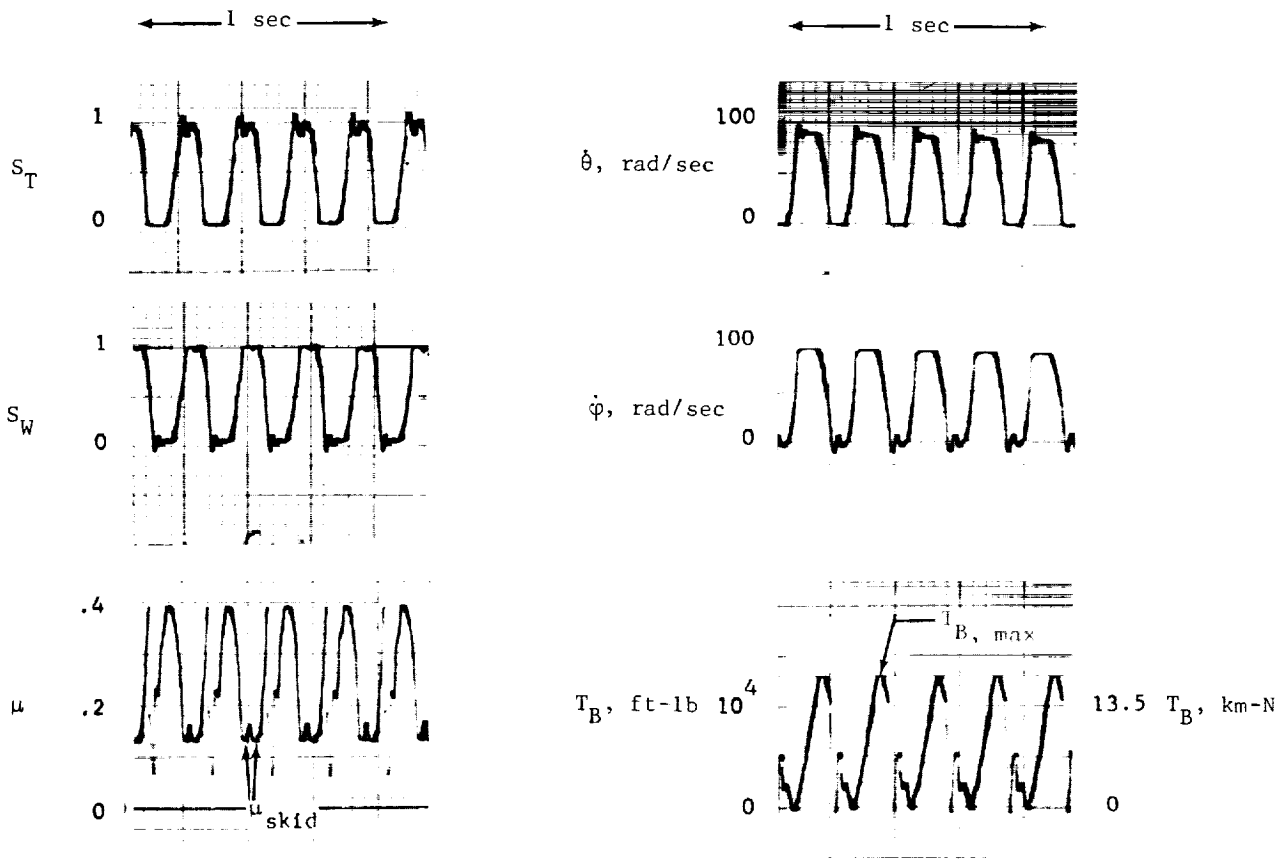
(a) $\ddot{\beta}_1 = 0$; $\ddot{\beta}_2 = -30$ radians/second²; $t_1 = t_2 = 0.1$ second; $\frac{\omega_{h,\beta}}{2\pi} = 0.5$ cycle/second; $\mu_{max} = 0.4$.

Figure 6.- Analog computer time-history solution.



(a) Concluded.

Figure 6.- Continued.



(b) Enlarged section from figure 6(a).

Figure 6.- Concluded.

COMPUTATIONAL PROCEDURE

Physical Constants

As indicated previously, the analog computer was programed to solve the dynamic equations of the braking system for a specific wheel, tire, and brake combination. The initial condition of forward speed of 200 feet per second (60.96 m/sec) was the same for all runs. Physical constants were chosen to describe a 32×8.8 type VII 22 ply rating tire and wheel combination. These constants are given in table I. This particular wheel and tire size was used because a large amount of braking data has been obtained for this combination at the Langley landing-loads track (ref. 6). It should be pointed out that the value of 1.16 feet (0.3536 m) chosen for r_{T1} was an average of the unbraked tire-rolling radius and the deflected radius. For this tire, the unbraked rolling radius for a vertical load of 22,000 pounds (97,856 N) is 1.22 feet (0.3719 m), whereas the deflected radius at this load is 1.10 feet (0.3353 m). The value of the torsional spring constant of the tire k_T was obtained from the empirical formula presented in reference 7.

TABLE I.- BRAKING-SYSTEM CONSTANTS

Tire radius, r_T , ft (m)	1.16	(0.3536)
Tire moment of inertia, I_T , ft-lbf-sec ² (kg-m ²) . . .	1.875	(2.542)
Tire spring constant, k_T , lbf/ft (N/m)	120,000	(175,080,000)
Tire damping ratio, ξ_ϕ	0.1	
Wheel radius, r_W , ft (m)	0.713	(0.2173)
Wheel moment of inertia, I_W , ft-lbf-sec ² (kg-m ²) . .	0.855	(1.1592)
Maximum brake torque, $T_{B,max}$, ft-lbf (m-N)	13,400	(18,167.72)
Vertical load, W , lbf (N)	20,000	(97,856)
Initial horizontal velocity, \dot{x}_O , ft/sec (m/sec) . . .	200	(60.96)
Sensor control damping ratio, ξ_β	0.7	

Test Variables

The test program consisted of obtaining computer solutions for some selected values of the brake time response t_1 and t_2 , the control acceleration at which brakes were applied and released $\ddot{\beta}_1$ and $\ddot{\beta}_2$, and the angular accelerometer control frequency $\omega_{n\beta}$. Certain combinations of these variables were used with the maximum coefficient of friction μ_{max} between tire and runway varying over a range from 0.1 to 0.8. The control accelerometer damping coefficient ξ_β was 0.7 for all runs. The range of the brake and control parameters investigated was restricted because the number of these variables and the possible combinations of these variables, even though confined to a practical range, would involve a formidable computer program if expanded to any extent. Because of the preliminary nature of this study, it was felt advisable to limit the scope of the investigation to a minimum number of solutions.

Accuracy Checks

In order to eliminate errors arising from unintentional circuitry changes and computer malfunctions, a series of frequency-response checks were carried out on individual components of the program each day, and also as a final check a standard test condition was run through the computer prior to each day's operation. The standard test condition incorporated the initial conditions and constants presented in table I. The other parameters associated with this run were

$$\mu_{max} = 0.4$$

$$t_1 = 0.1 \text{ sec}$$

$$t_2 = 0.1 \text{ sec}$$

$$\frac{\omega_{n,\beta}}{2\pi} = 0.5 \text{ cps}$$

$$\ddot{\beta}_2 = -30 \text{ rad/sec}^2$$

$$\ddot{\beta}_1 = 0 \text{ rad/sec}^2$$

The time-history traces of the computer outputs obtained for the standard run are shown in figure 6(a). Use of the standard run in checking consisted of a visual comparison of each channel with the corresponding channel of a master standard run. In addition, the values obtained for the total runout x and the total work done in skidding W_{skid} were found to check the master values within about 2 percent when everything was operating properly.

The saw-toothed appearance of x , the forward displacement time history, resulted from the method programed to obtain a maximum output sensitivity from this channel. For this channel, the maximum galvanometer displacement was set to represent 100 feet (30.48 m) of displacement, and as each 100-foot (30.48-m) segment was traversed, the output polarity was reversed so that the saw-tooth record was obtained. Total displacement is obtained by multiplying the number of lines connecting the upper and lower peaks (in this case 20) by 100 and then adding the proportional deflection of the last partial-line segment. For the record shown in figure 6(a), the total runout was 2,075 feet (632.46 m).

For these runs the computer was slowed down so that its actual speed of operation was 1/20th of real-time operation speed. This time scaling was necessary because the frequency response demanded of the computer in solving this problem was greater than its capability in real time.

During some of the runs, selected outputs were recorded by a mechanical X,Y plotter. In order to insure that the inertias of the X,Y-plotter components were not attenuating the plotted results, the plots were compared with observations made of the identical run using a cathode ray oscilloscope.

Calculation of Braking-System Efficiency and Skid Index

Some results of the computer program are discussed in terms of braking-system efficiency and also in terms of the braking-system skid index. Efficiency η is defined herein as the ratio of the minimum stopping distance to the actual stopping distance multiplied by 100 to express it in percent. The minimum stopping distance depends on the initial velocity and the value of μ_{max} . The actual stopping distance is the final value of x obtained from the computer. Expressed symbolically, the efficiency is

$$\eta = \frac{\frac{\dot{x}_0^2}{2} \mu_{\text{max}} g}{x} \times 100$$

Skid index σ is defined as the ratio of the total work done in skidding to the initial kinetic energy of the airplane multiplied by 100 to express it in percent. Expressed symbolically, the skid index is

$$\sigma = \frac{W_{\text{skid}}}{\frac{Wx_0^2}{2g}} \times 100$$

The work done in skidding can be obtained from the computer results by using equation (9), and the initial kinetic energy depends on the initial airplane velocity and weight. This parameter is a measure of the amount of total stopping energy contributed by skidding of the tire. It then follows that for optimum operation of braking systems, the efficiency should be as large as possible and the skid index as small as possible.

RESULTS AND DISCUSSION

The results and discussion are presented in two parts: The first part deals with the effects of tire elasticity, brake time response, and control frequency on the braking system when the available tire-runway friction coefficient is large enough to be comparable with the coefficients encountered during landing stops on most dry or damp runways. The magnitude of the coefficient used, however, is low enough to permit the maximum brake torque to lock the wheel; that is, $T_{B,\text{max}} > \mu_{\text{max}} W r_T$. The second part discusses the effect of lower friction coefficients on the braking systems. Low coefficients may be experienced when runway surfaces are contaminated with foreign substances such as water, slush, snow, and ice.

Large Tire-Runway Friction Coefficients

Effect of tire elasticity on wheel motion.- As was mentioned earlier when tire torsional elasticity is considered, the wheel motion may differ from the motion of the tire in the ground-contact area. This condition is particularly true when brake torque is being cycled at a rapid rate. The significance of this differential motion between the wheel and tire lies in the fact that the skid-control sensor is mounted on the wheel whereas the vehicle retarding force is developed in the tire footprint and as pointed out previously, this force depends on the tire motion. Therefore, the control- and brake-response frequencies must be chosen so that the applied brake torque controls the tire motion in the desired manner even though the brake-control signals depend on the wheel motion.

An example of the character of the individual motions of the wheel and the tire during cyclic braking can be seen in the standard run record presented in figure 6. During this run, brake torque was cycled at a fairly rapid rate by the control and complete wheel locking begins after a runout of about 1,000 feet (304.80 m). In this region the wheel angular velocity $\dot{\theta}$ reaches zero and the

wheel remains locked for a brief period of time, (approximately 0.2 second); then as the brake torque drops off, it rapidly returns to the free-rolling condition. This condition of wheel locking followed by free rolling then continues in a cyclic manner throughout the remainder of the run. During the first 1,000 feet (304.80 m) of the runout, however, the wheel angular velocity was large enough to make the response of the accelerometer control and brake adequate to prevent complete locking. Although complete locking did not occur in the first 1,000 feet (304.80 m), it can be seen that both the wheel and tire slip-ratio traces indicated a significant amount of wheel and tire slip.

The character of the relative motion between the wheel and tire can be observed by comparing the wheel and tire angular velocity traces $\dot{\theta}$ and $\dot{\phi}$ in figure 6 during the period of wheel locking and spin-up. It can be seen from the $\dot{\phi}$ trace that the tire angular velocity becomes oscillatory and even exhibits negative values (rearward rotation) during some instants while the wheel is fully locked, that is, $\dot{\theta} = 0$; or in other words, after the wheel came to a complete stop, the tire made several torsional oscillations about the axle center line. The oscillation in $\dot{\phi}$ while $\dot{\theta}$ has a zero value is a result of tire elasticity and tire inertia and can be seen on the tire slip-ratio trace S_T as an oscillatory variation which takes on values greater than 1 when the tire angular velocity is negative. The foregoing results indicate differences between wheel and tire motion when the wheel is locked and wheel and tire slip ratios have values in the neighborhood of 1.

Differences between wheel and tire motion due to the elastic behavior of the tire can also be seen at the other end of the slip-ratio scale, that is, when S_W and S_T are in the neighborhood of zero. For this condition, however, the wheel slip-ratio trace S_W indicates that the slip ratio of the wheel takes on negative values, whereas the tire slip ratio is never less than zero. This result indicates that during wheel spin-up, the spring force developed by the tire drove the wheel to angular velocities greater than those corresponding to that required for free rolling at the forward speed \dot{x} . This phenomena of wheel angular velocity having larger values just after spin-up than it had prior to wheel locking is often observed during both landing-loads track and dynamometer-braking tests. It should be stated, however, that during actual braking tests, tire stretch occurring during the application of drag load also adds to this effect.

The overall effect of differences in wheel and tire motion on the variation of μ with slip ratio throughout the entire slip-ratio range can be seen in figure 7. These curves (fig. 7) were obtained during the braking stop shown in figure 6 by connecting the computer outputs of friction coefficient and slip ratio to a mechanical X,Y plotter where μ was plotted against slip ratio. The plot on the right shows the programmed variation of μ with S_T and remained unchanged throughout the entire landing run; the plot on the left, however, which indicates the variation of μ with S_W , exhibits significant variations from cycle to cycle. It is of particular significance to note that the slope of the curve of μ plotted against S_W can have either positive or negative values when the value of $S_T = 0$. This result is in contrast to current notions regarding this variation since experimental data for μ plotted

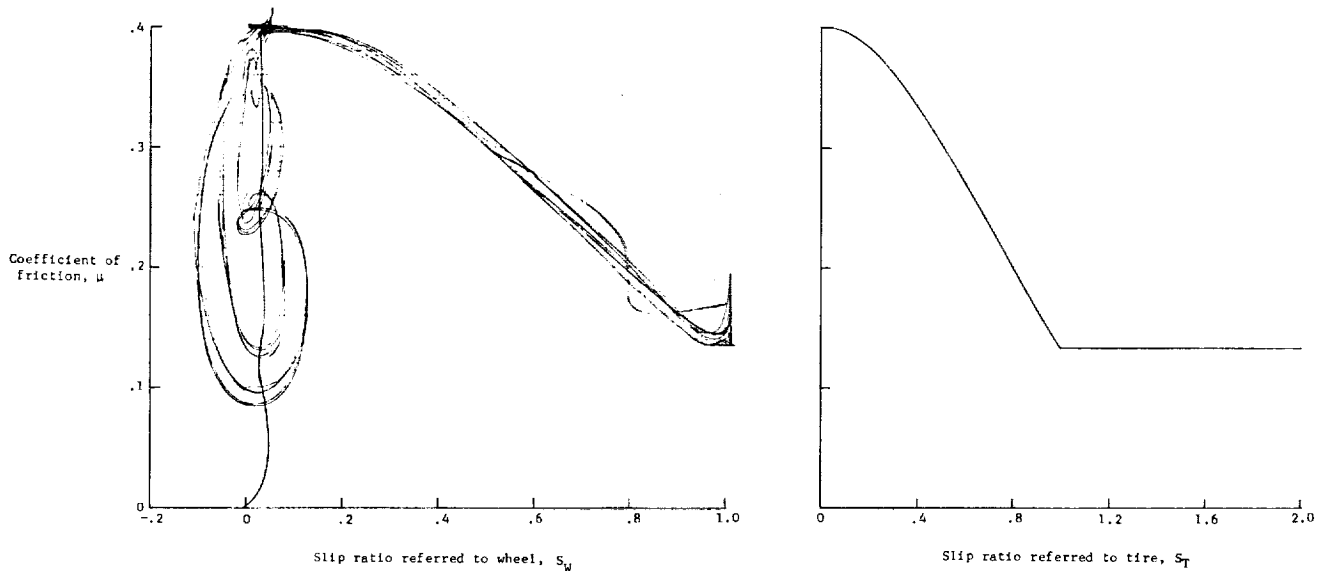


Figure 7.- Analog computer outputs obtained over a large number of braking cycles showing variation of friction coefficient with wheel and tire slip ratios. Data obtained from test shown in figure 6.

against slip is normally presented with this slope drawn positive. This result would indicate that for the conditions of this run, a control sensor located on the wheel could not be used to determine whether the tire is operating in the range between free rolling and μ_{\max} or between μ_{\max} and the locked-wheel condition, just on the basis of the slope of the μ -slip curve for the wheel.

Effect of tire elasticity on coefficient of friction.- Another aspect of tire elasticity is indicated in the coefficient of friction trace appearing in figure 6. During the time that the wheel is locked, the coefficient of friction is substantially constant and equal to μ_{skid} except for a small spike caused by the tire oscillation. When the brake torque drops to a value which is low enough to permit the wheel to start turning, the value of μ rises very rapidly. This rapid rise is caused by the increase in the spin-up drag load as the tire goes from a full-slip to a zero-slip condition during the time that the brake torque is decreasing; that is, at the instant the wheel starts turning, the spin-up drag load is equal to $\mu_{\text{skid}}W$, and as the brake torque continues to decrease, the drag load increases until its value is $\mu_{\max}W$ at the instant the tire slip ratio S_T reaches zero. It is of interest to note that for the conditions of this run, the time period required for the wheel to spin up from its fully locked condition to free rolling was somewhat less than the time period required to go from the initial incipient skid condition to a fully locked wheel condition. This fact can be observed by comparing the slopes of both the μ and $\dot{\theta}$ time-history curves during spin-up and spin-down.

Immediately upon reaching μ_{\max} after spin-up, it can be seen that the value of μ drops very rapidly toward zero. The decrease is so rapid that the record trace becomes much less pronounced because of the higher galvanometer writing speed. The time rate at which μ decreases in this run depends almost entirely on the natural period of the tire. It is evident from figure 6(b) that the coefficient of friction did not return to a zero value prior to the start of the next cycle. The reason for this effect was that even though this was a short period of time, it was long enough for this control and brake to reapply a sufficient amount of brake torque to prevent the friction coefficient from reaching a value of zero.

The fact that the value of the coefficient of friction is affected by the response period of the tire indicates that the stopping distances would also be affected by tire elasticity. From a practical standpoint, this result would indicate that the same brake and control system could exhibit different stopping efficiencies when used with wheel and tire combinations having different torsional frequencies.

Control-sensor and brake-time response.- Figure 8 shows the effect of variation of the accelerometer-control frequency on braking-system efficiency for

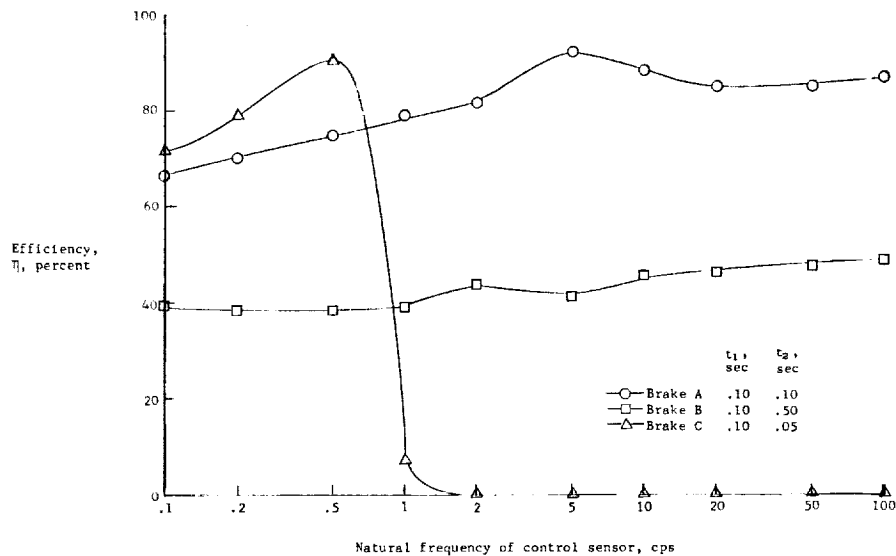


Figure 8.- Variation of braking-system efficiency with sensor-control frequency for three brakes having different torque decay rates. $\beta_1 = 0$; $\beta_2 = -30$ radians/second²; $\mu_{\max} = 0.4$.

three brakes A, B, and C which differ from each other only in their response times. The time for brake torque to rise from 0 to the limiting value of 13,400 foot-pounds (18,167.72 m-N) was 0.1 second for all three brakes and the value chosen for μ_{\max} was 0.4 for all the runs. Also for all three brakes the acceleration value that caused a brake release signal to be generated was -30 radians per second per second, and for brake application, zero radians per

second per second. For each brake, however, the time required for the torque to decrease from its maximum value to zero was different; that is, for brake A, $t_2 = 0.1$, for brake B, $t_2 = 0.5$, and for brake C, $t_2 = 0.05$. The lowest value of brake decay time was used with brake C and is fairly representative of the fastest rate of brake release obtainable with current brakes. Although data on brake-response time are very scarce, it appears that modern brakes do not operate at frequencies much greater than 10 cycles per second.

It can be seen in figure 8 that brake A reached a peak efficiency of 92 percent when operated by a control having a frequency of about 5 cycles per second. The lowest efficiency for brake A of about 67 percent occurred at the lowest control frequency used for these calculations, that is, 0.1 cycle per second. Brake B shows a much smaller variation in efficiency throughout the control frequency range but its maximum value is significantly lower than that of brake A. The maximum efficiency of 49 percent for brake B occurs at the highest control frequency which was 100 cycles per second. Brake C exhibits the highest efficiency of all three brakes in the lower control frequency range; its efficiency rises from a 71-percent value at a control frequency of 0.1 cycle per second to about 90 percent at 0.5 cycle per second. When, however, the control frequency is increased beyond 0.5 cycle per second, the efficiency drops off very rapidly to a negligible value and indicates a complete loss in stopping ability. The reasons for the behavior of brakes A, B, and C, as shown in figure 8, can be explained by the computer time-history records obtained for some of the runs.

Figure 9 shows the time histories obtained for brake A with an accelerometer-control frequency of 5 cycles per second, the condition of maximum efficiency for this brake. At the start of the braking cycle, it can be seen that the control acceleration values β are oscillating very rapidly and the frequency of this oscillation is about 90 cycles per second. Furthermore, the brake torque time-history trace indicates that the control must be generating brake application and release signals since the brake torque never reaches its limited value. Therefore, the values of β must cover the range between 0 and -30 radians per second per second. Since the ratio of the frequency at which the accelerometer exercises control to its natural frequency is about 18 and thus would result in large attenuation to its response, it follows that the wheel accelerations θ which drive the accelerometer must be extremely large. This high-frequency control response enables the relatively low-frequency accelerometer to exercise precise, or very high response, control of the braking cycle, as will be shown shortly. It should be pointed out, however, that this response is dependent on the shape of the time variation in brake torque; that is, if a more gradual or curved characteristic of torque plotted against time at the instant of application and release of brake torque had been used, the resulting values of θ might not have been high enough to drive the accelerometer to the amplitudes required for brake control. Since the control is set to apply brake torque at zero angular acceleration and release it at -30 radians per second per second, brake torque is being applied over a larger part of each control cycle; therefore, the brake torque increases at the start of the run until the tire is operating at the maximum friction coefficient. From this point on, the tire begins to slip but since, as was just mentioned, the control is capable of very high response, this condition

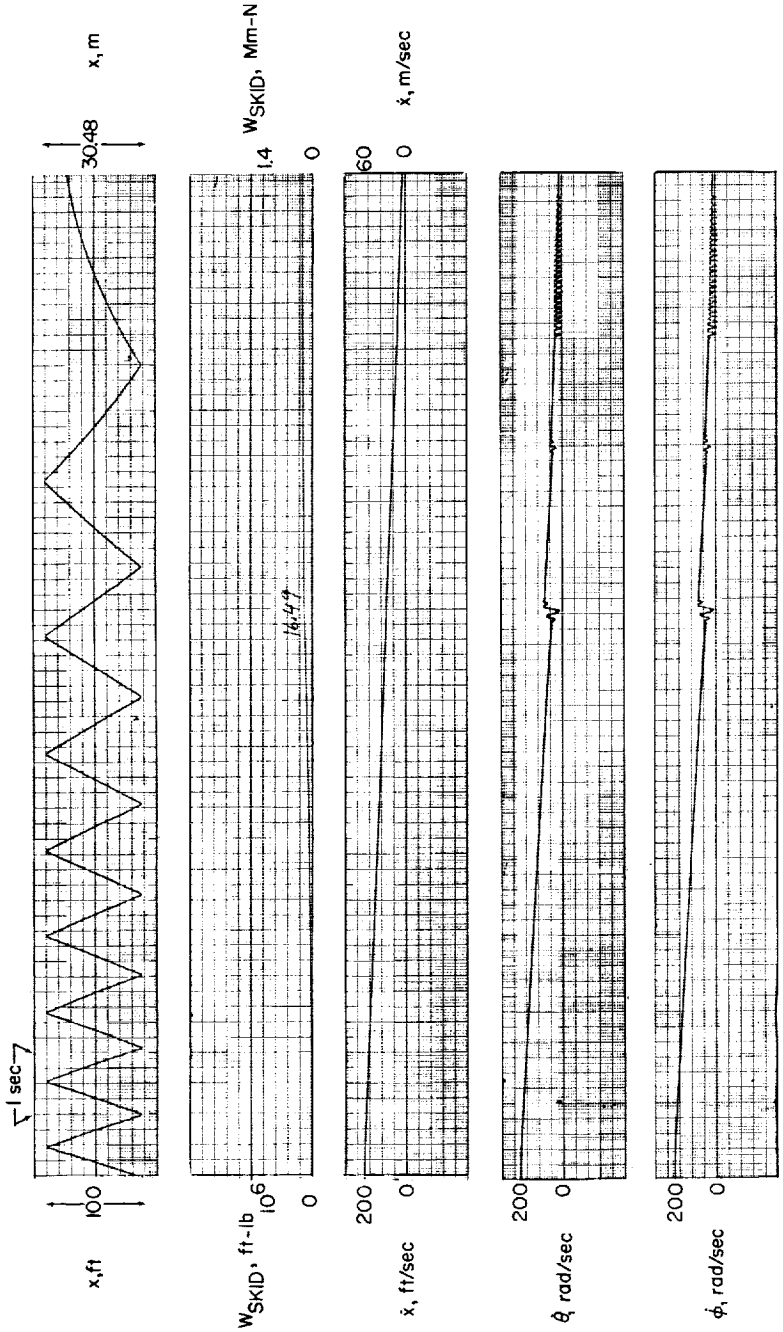


Figure 9.- Analog computer time-history solution using brake A. $\ddot{\beta}_1 = 0$; $\ddot{\beta}_2 = -30$ radians/second²;

$$t_1 = t_2 = 0.1 \text{ second}; \frac{\omega_h, \beta}{2\pi} = 5 \text{ cycles/second}; \mu_{\max} = 0.4.$$

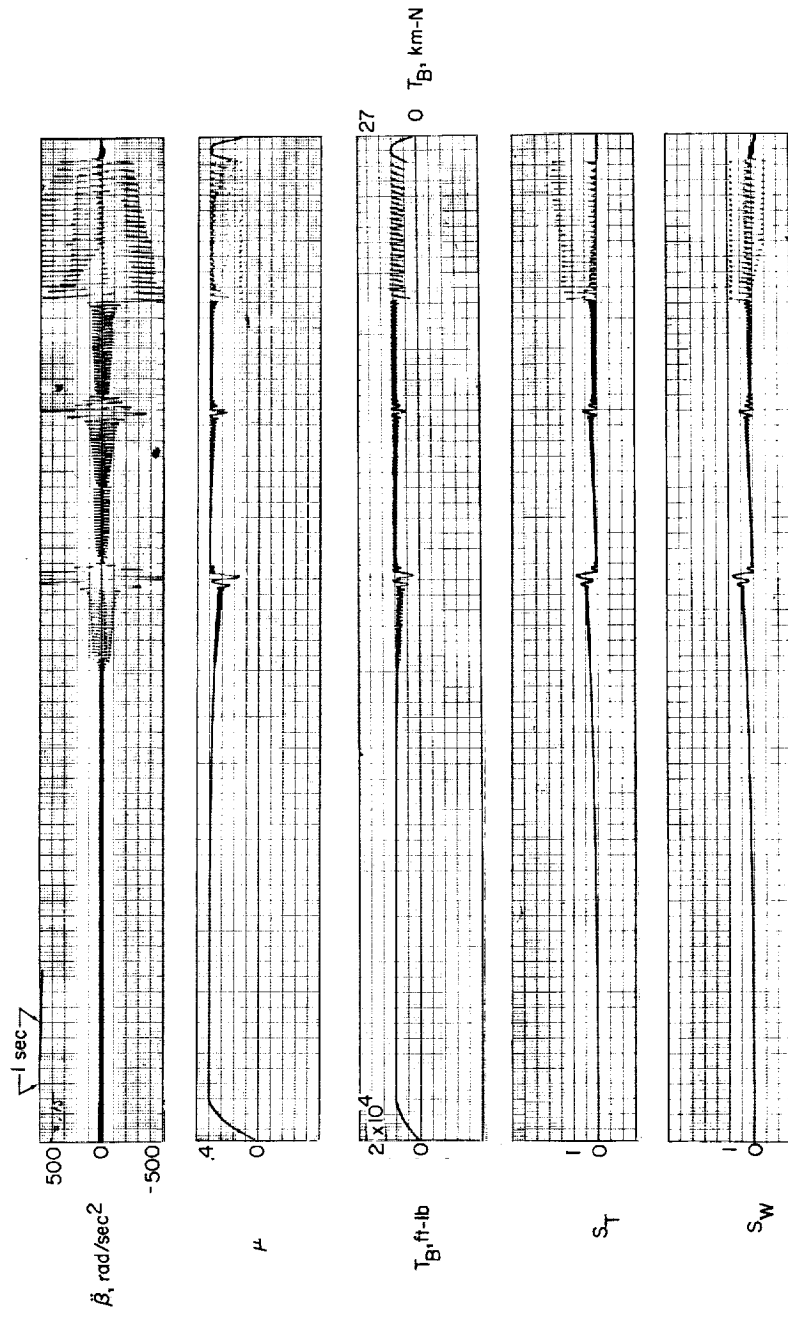


Figure 9.- Concluded.

prevents immediate lock-up of the wheel and, as indicated by the S_T time-history curve, controls the braking smoothly even though the tire is slipping. At the small slip ratios, control is well within the capabilities of the braking system since the slope of the μ -slip curve for the tire is also small. As the slip ratio increases, however, the slope of the μ -slip curve for the tire increases and tends toward a more unstable condition. (See fig. 3(a).) It can be seen that the accelerometer loses its ability to control the system smoothly when the tire slip ratio reaches a value of around 0.5. At this point, the entire character of the time histories are changed and the wheel and tire spin back up, and the cycle is repeated until a low rolling speed is reached.

The decrease in efficiency for brake A, shown in figure 8, at the higher control frequencies is caused by the higher frequency accelerometer being capable of exercising smooth control over a larger portion of the back side of the μ -slip curve. Therefore, the tire operates at higher slip ratios and at correspondingly lower coefficients of friction for a somewhat larger part of the run before instability occurs. This effect can be seen in figure 10 which shows the time histories obtained for brake A with a control accelerometer frequency of 50 cycles per second.

The lower values of efficiency obtained for brake A at the lower control frequencies is basically caused by the low response of the accelerometer. It can be seen in figure 6(a), which is the computer run made by using brake A and a control frequency of 0.5 cycle per second, that the time between brake-release signals, as indicated by the β trace and T_B trace, is about 0.2 second. This comparatively long time period allows the brake to lock the wheel and therefore causes the tire to operate at the full skid coefficient μ_{skid} throughout a large proportion of the run. Since μ_{skid} is a relatively low-friction value, the efficiency of the braking system is degraded. Although the motion β of the control is very complex and depends on the coupled response of the various masses and elastic properties of the system, a coarse physical understanding of the underlying reason for the very low response of the 0.5-cycle-per-second accelerometer as compared with the 5-cycle-per-second control can be obtained from figure 11. Figure 11 shows the variation of $\beta - \theta$ as a function of control natural frequency for the case of simple harmonic motion in which the maximum acceleration is 30 radians per second per second. It can be seen that for a natural frequency of 0.5 cycle per second, the angular displacement must be around 170° whereas for a natural frequency of 5 cycles per second, the excursion is less than 2° .

The consistently low values of efficiency (between 40 percent and 50 percent) exhibited by brake B throughout the range of control frequencies are due primarily to the relatively long brake release time $t_2 = 0.5$ second. Figure 12 shows the time histories of the run made with this brake by using a control frequency of 5 cycles per second. At the start of braking, the control causes the system to reach μ_{max} rapidly for much the same reason as described for brake A operating at this same control frequency. The rise in torque for this brake is actually faster than that for the equivalent brake A. The reason, of course, being that brake torque decayed at a much slower rate following the generation of a release signal. This slow rate of brake decay

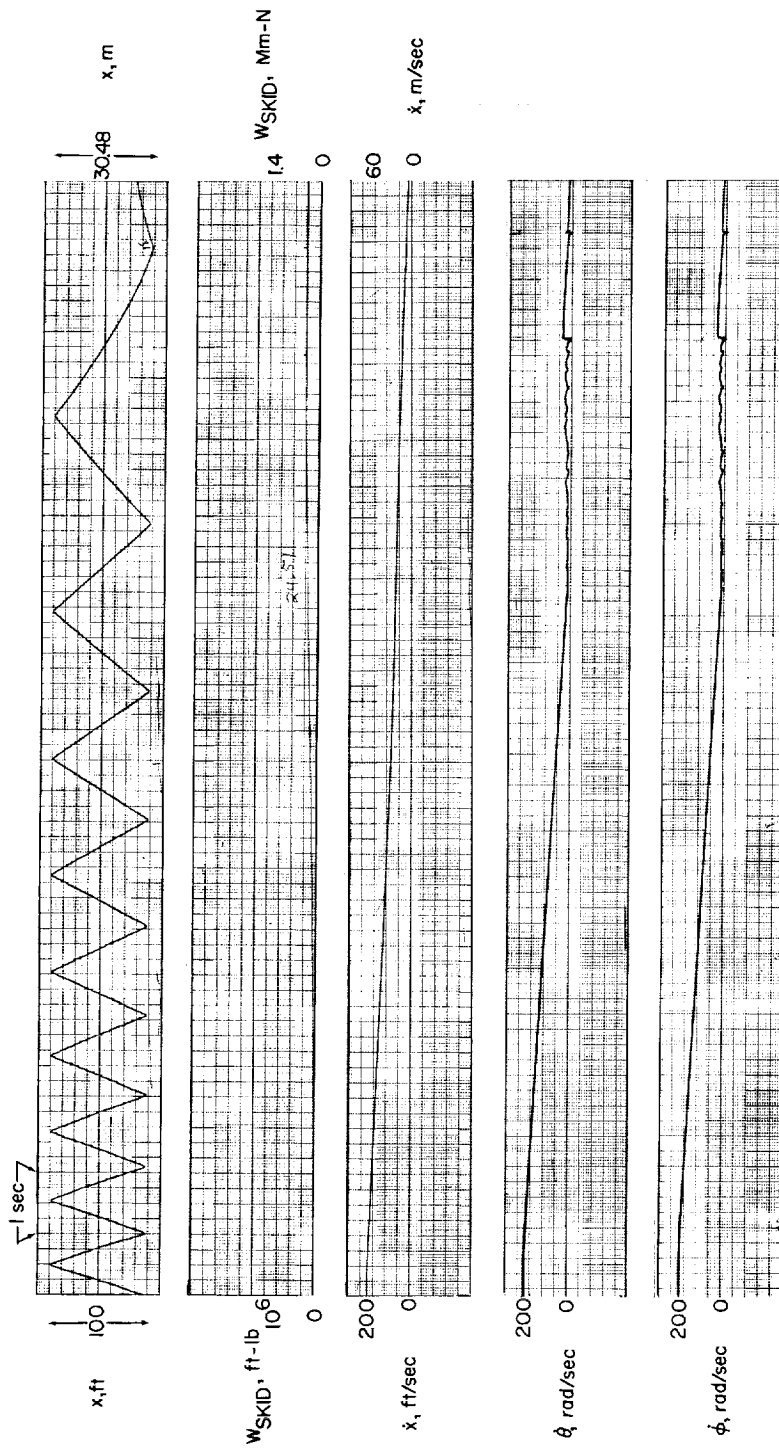


Figure 10.- Analog computer time-history solution using brake A. $\ddot{\beta}_1 = 0$; $\ddot{\beta}_2 = -30$ radians/second²;
 $t_1 = t_2 = 0.1$ second; $\frac{4h_1\beta}{2\pi} = 50$ cycles/second; $\mu_{\max} = 0.4$.

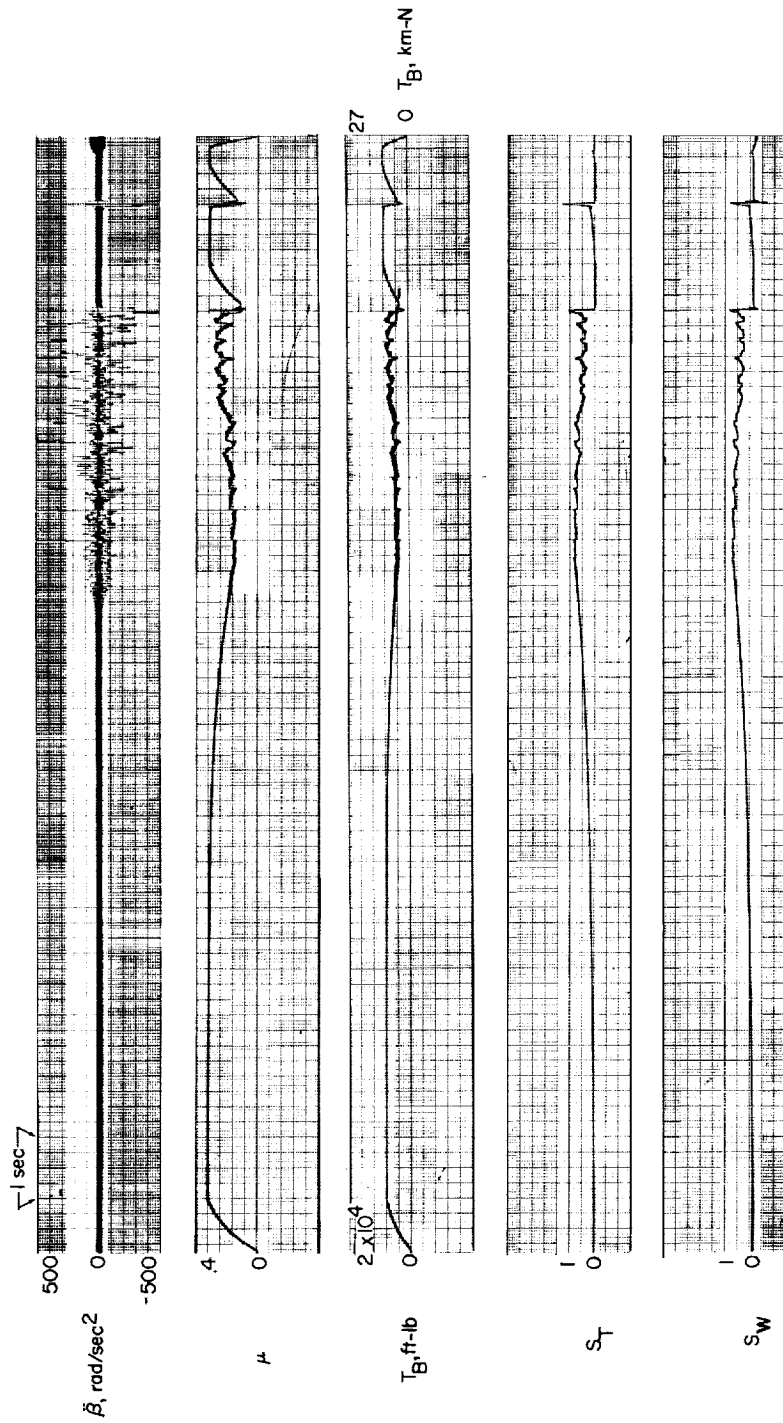


Figure 10.- Concluded.

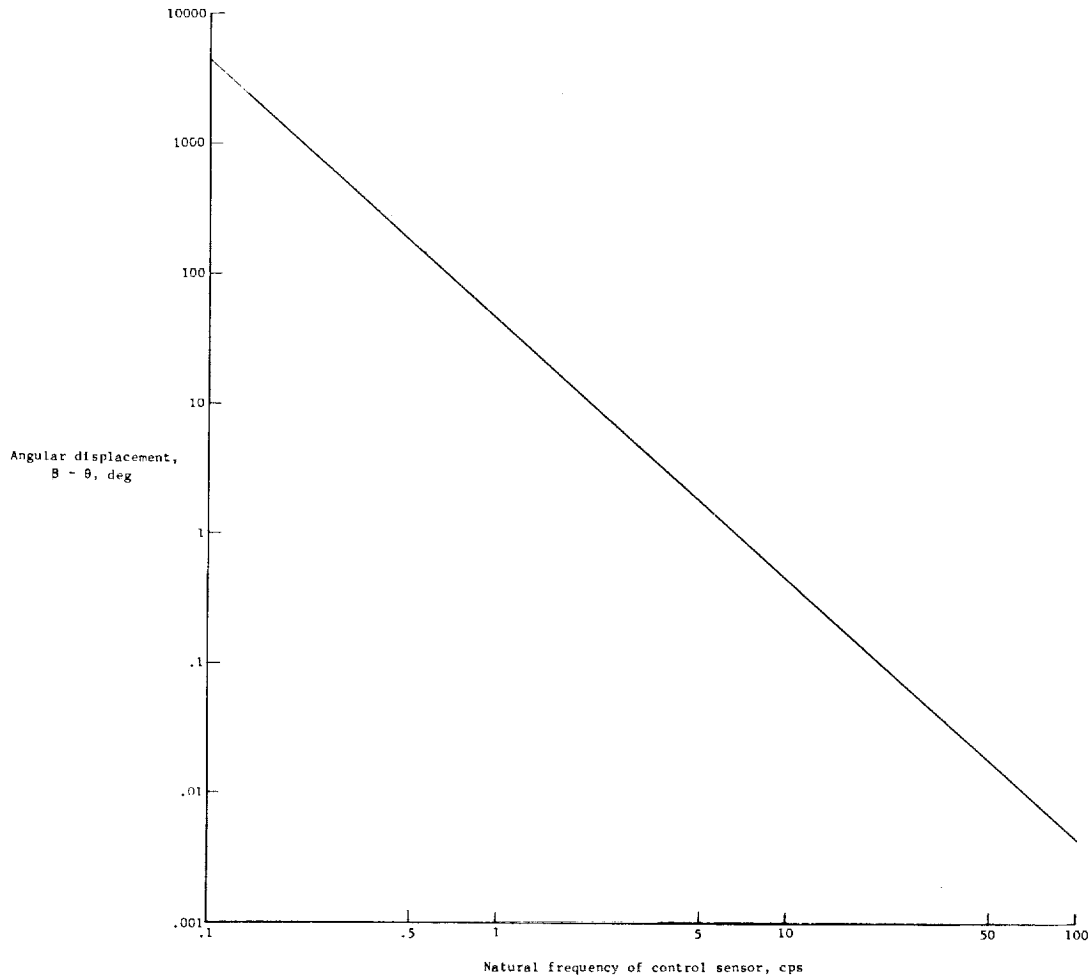


Figure 11.- Variation of angular displacement, of sensor control mass with respect to wheel, with natural frequency of sensor control for the condition of simple harmonic motion and maximum sensor angular acceleration of 30 radians/second².

also prevented the accelerometer from exercising precise control at values of $S_T > 0$; therefore, the wheel reached a full-skid condition in a relatively short period of time as compared with that for the equivalent brake A. Furthermore, the tire was not able to return to the nonslip condition after reaching full skid because of the slow brake-torque decay rate, and thus operated at or near μ_{skid} throughout the remainder of the run. It should be pointed out that for this portion of the run, the brake release signals were probably generated by the low wheel speed control.

The very different variation of brake C with control frequency as compared with the other braking systems is basically due to the brake decay time t_2 being significantly less than the application time t_1 . Figure 13 shows the run made with this brake at a control frequency of 0.2 cycle per second.

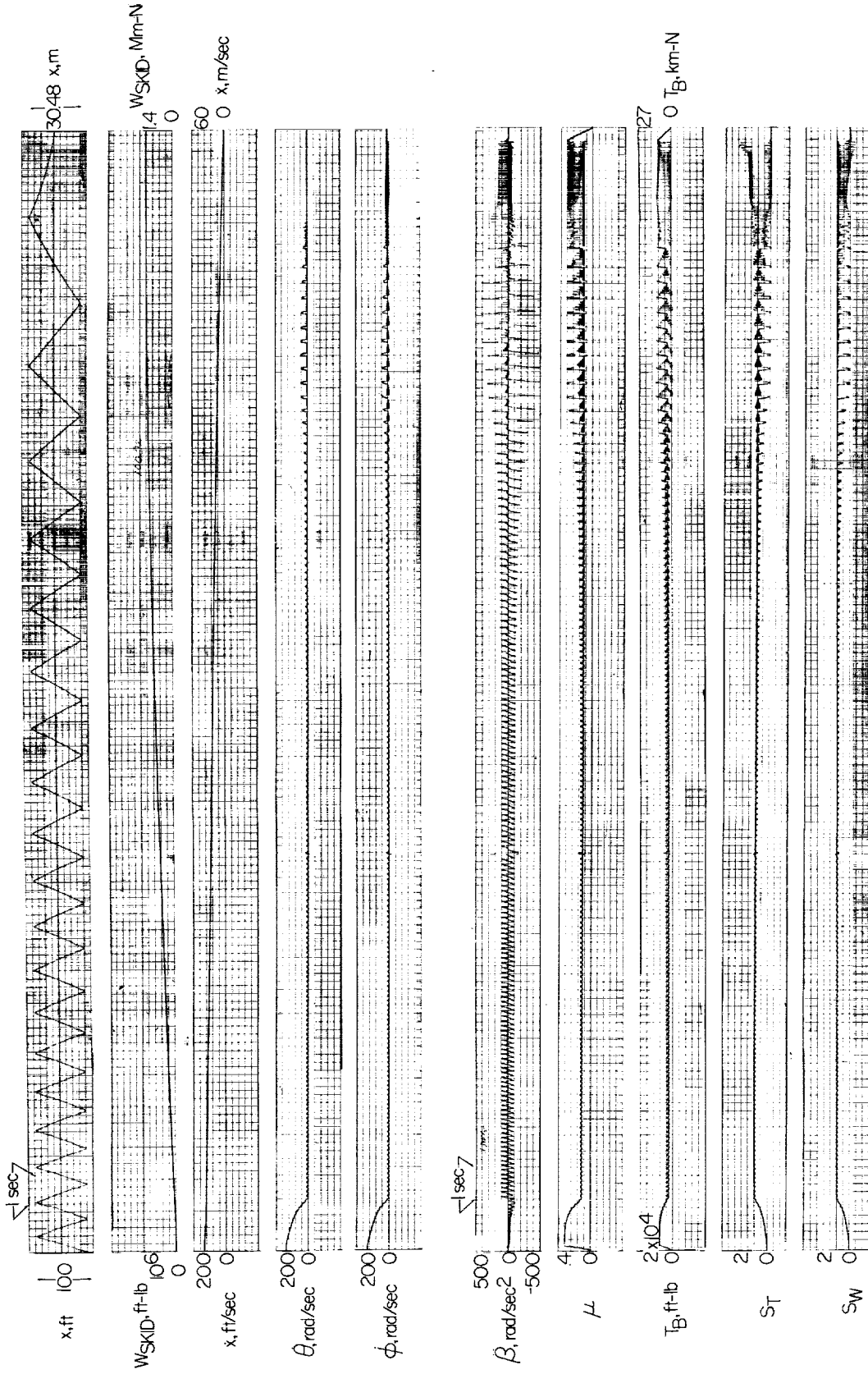


Figure 12.- Analog computer time-history solution using brake B. $\ddot{\beta}_1 = 0$; $\ddot{\beta}_2 = -30$ radians/second²; $t_1 = 0.1$ second;

$$t_2 = 0.5 \text{ second; } \frac{u_n, \beta}{2\pi} = 5 \text{ cycles/second; } \mu_{max} = 0.4.$$

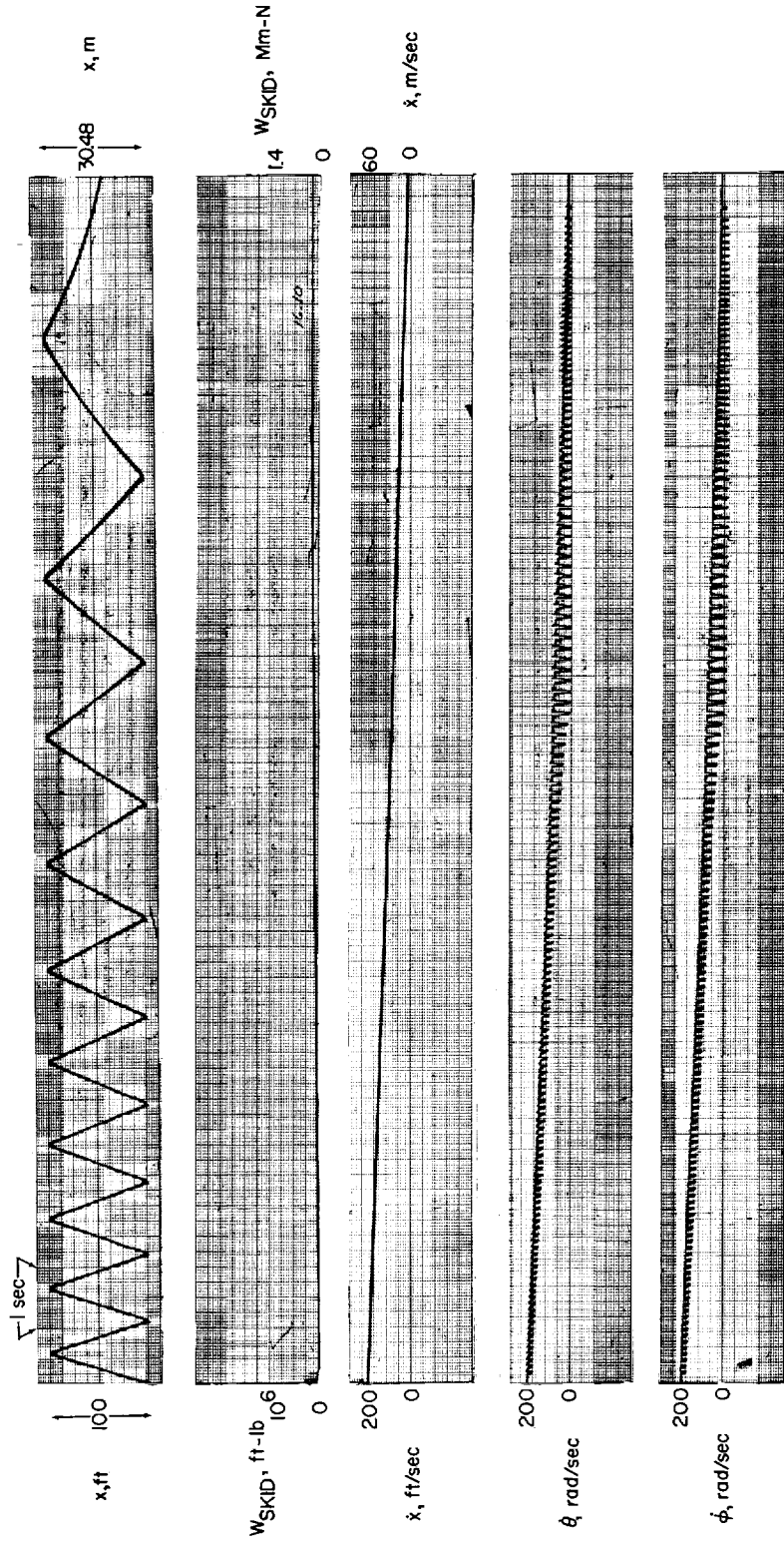


Figure 13.- Analog computer time-history solution using brake C. $\ddot{\beta}_1 = 0$; $\ddot{\beta}_2 = -30$ radians/second²; $t_1 = 0.1$ second;

$$t_2 = 0.05 \text{ second}; \frac{\omega_{\beta}, \beta}{2\pi} = 0.2 \text{ cycle/second}; \mu_{\max} = 0.4.$$

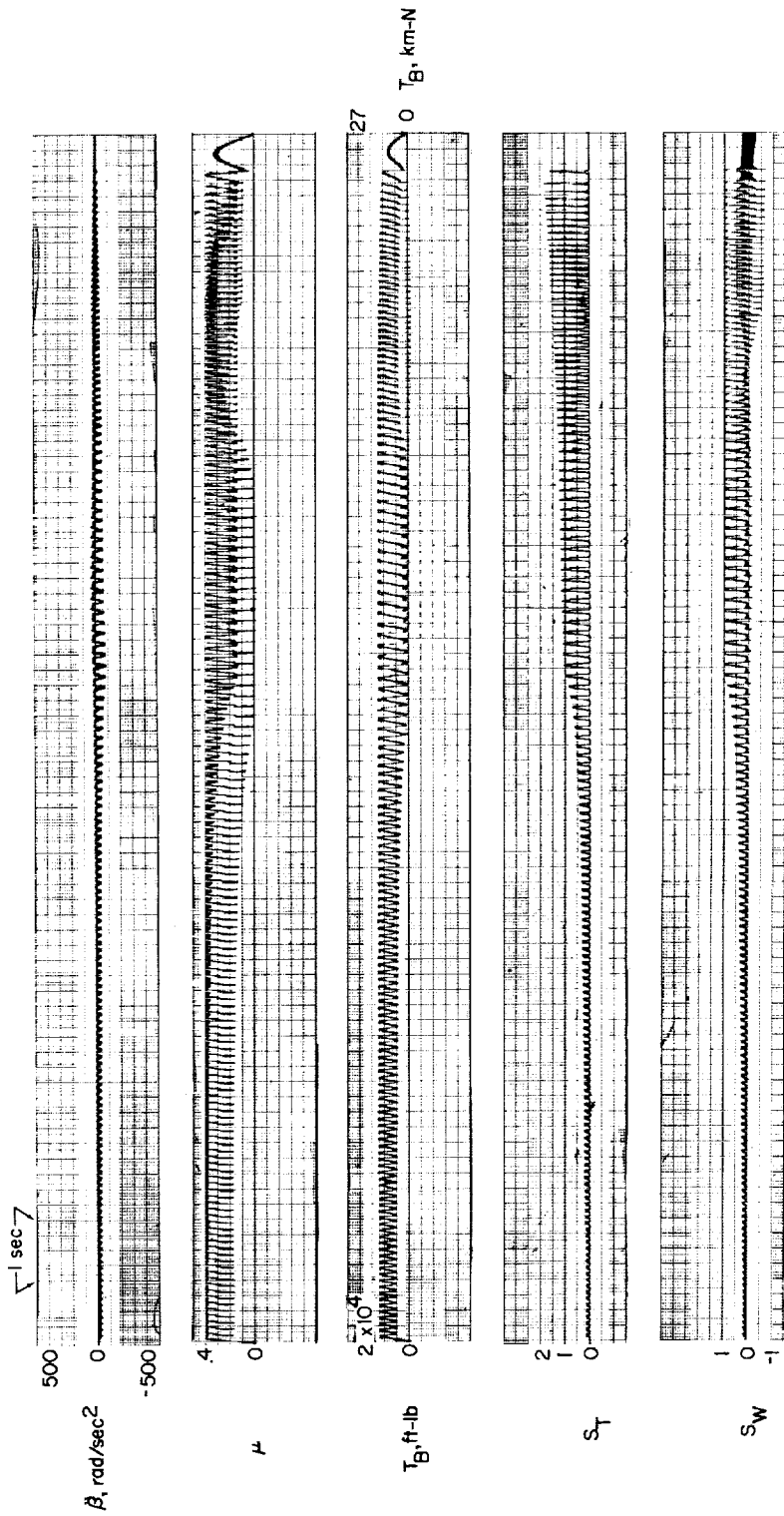


Figure 13.- Concluded.

The efficiency, as indicated in figure 8, was about 79 percent. This braking system operates around the peak of the μ -slip curve for the tire (fig. 3(a)), and for most of the run, the excursions on both sides of this optimum point persist for only a relatively short period of time. This fact can be noted on both the S_T and μ time histories. The μ time history indicates that with the exception of the last several hundred feet of the run, the friction coefficient was held at a value which averaged close to μ_{\max} . This condition was made possible because, despite the low response of the control, the wheel was capable of driving the control to sufficiently high values of acceleration to generate brake release and application signals about 10 times each second during most of the run. Furthermore, as can be seen in figure 13, the response of the control signal appeared as a distorted wave and its shape was such that brake torque was being applied during a greater portion of the time of each braking cycle. Despite the longer time of brake application, the tire was not able to reach a large value of slip ratio because of the rapid rate at which brake torque decreased once a release signal was generated. The highest efficiency obtained for brake C occurred at a control frequency of 0.5 cycle per second and was a result of this control generating more brake release signals per unit time than for the brake operating at 0.2 cycle per second; and thus the excursions of the friction coefficient on each side of the maximum were shortened. This effect can be seen in figure 14.

The very abrupt drop in braking efficiency that occurred when the control frequency was increased beyond 0.5 cycle per second again resulted from the fact that the amplitude response of this control to the wheel angular accelerations $\ddot{\theta}$ was sufficient to generate brake release signals at a very high frequency. Furthermore, these high-frequency control accelerations appeared as a fairly pure wave form, and since the brake torque decayed at double the rate at which it was applied, it was not possible for this system to develop any brake torque. This effect can be seen in figure 15 which shows only a short section of the run made with brake C at a control frequency of 10 cycles per second.

The foregoing discussion of figure 8 indicates that the efficiency of a braking system depends on a rather complex interaction between the values of tire frequency, brake response, control frequency, and the slope of the μ -slip curve for the tire. Since the combinations investigated indicated that the efficiency of braking systems could vary from more than 90 percent down to 0, this result would indicate the need for careful analysis and testing in the selection and integration of the individual hardware units which comprise the braking system. These results also indicate that under certain dynamic conditions, an accelerometer with a relatively low response can exercise precise control of brake torque over a large part of the back side of the μ -slip curve for the tire.

Low Tire-Runway Friction Coefficients

Causes of low friction coefficients.- As was indicated previously, current braking systems operate satisfactorily on dry or even damp runway surfaces. For these cases, substantial retarding forces can be developed by the braking

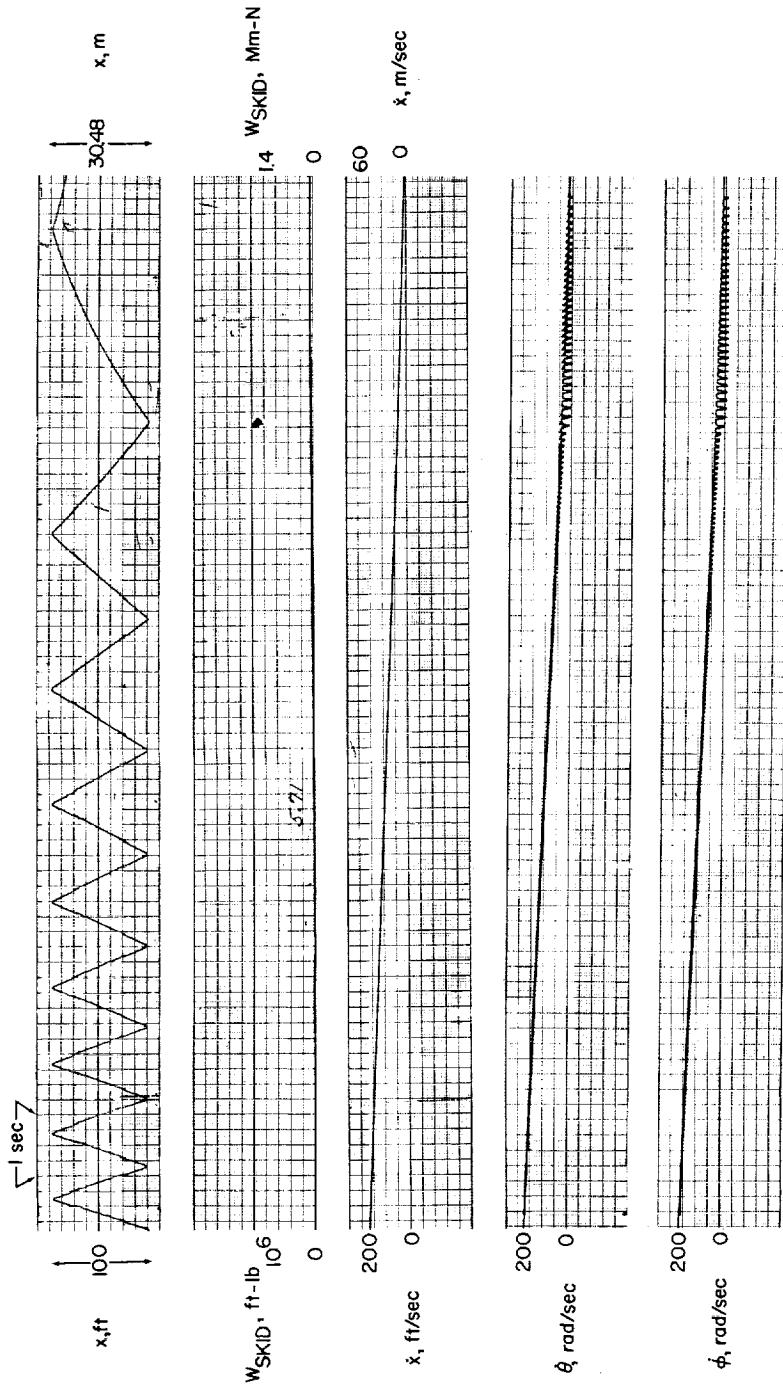


Figure 14.- Analog computer time-history solution using brake C. $\ddot{\beta}_1 = 0$; $\ddot{\beta}_2 = -30$ radians/second²;
 $t_1 = 0.1$ second; $t_2 = 0.05$ second; $\frac{\omega_{h,\beta}}{2\pi} = 0.5$ cycle/second; $\mu_{max} = 0.4$.

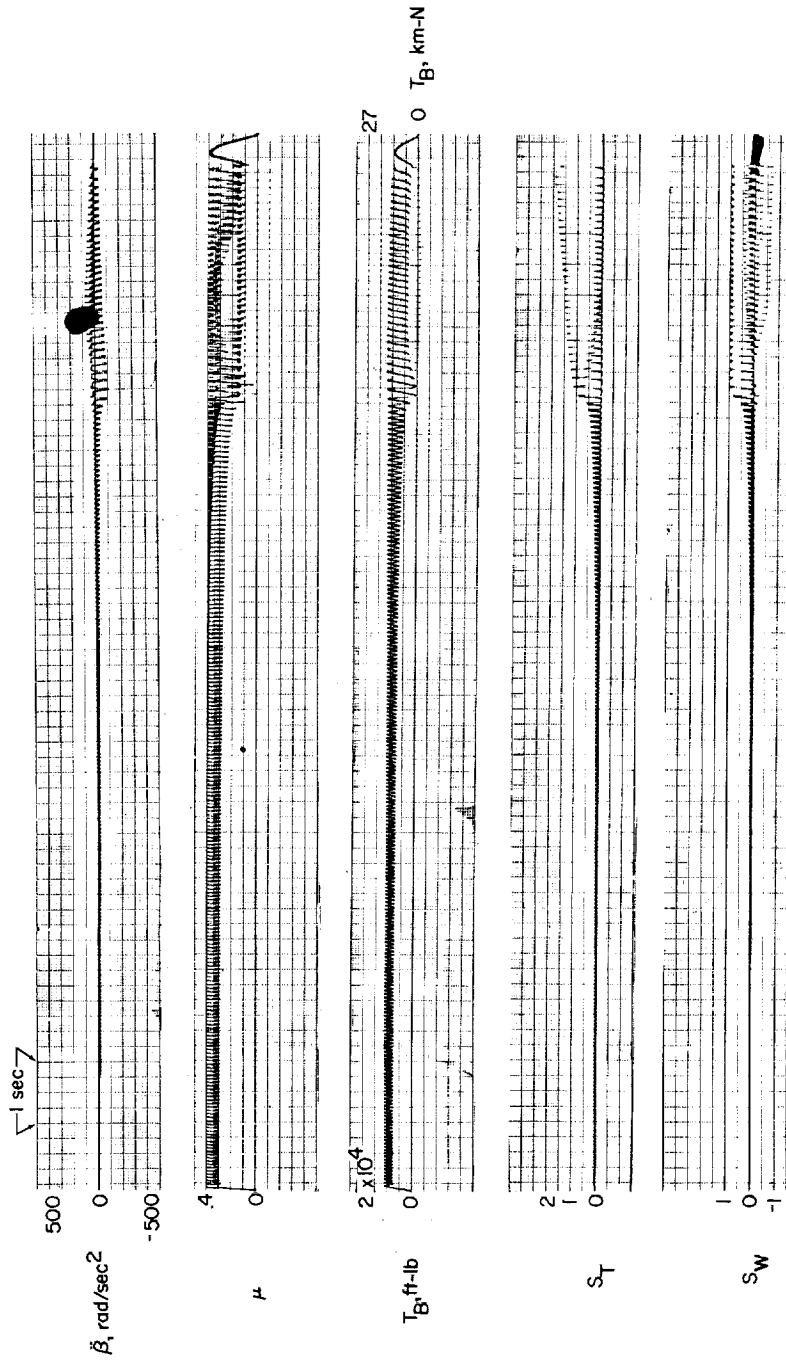


Figure 14. - Concluded.

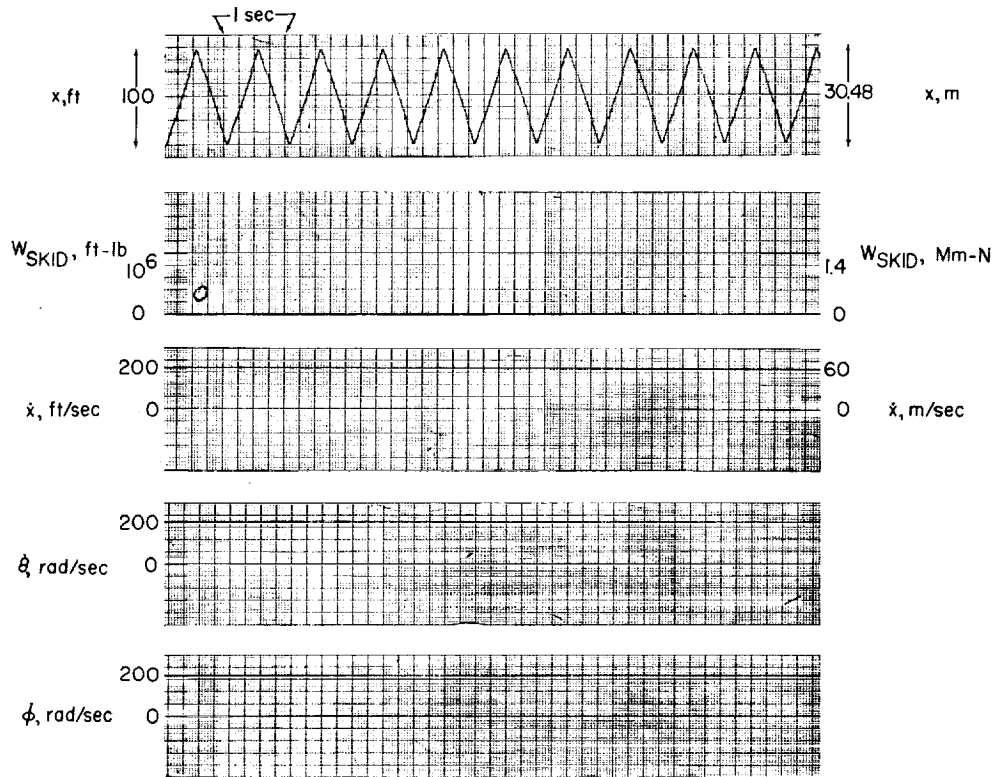


Figure 15.- Analog computer time-history solution using brake C. $\ddot{\beta}_1 = 0$;
 $\ddot{\beta}_2 = -30$ radians/second²; $t_1 = 0.1$ second; $t_2 = 0.05$ second;
 $\frac{\omega_{n,\beta}}{2\pi} = 10$ cycles/second; $\mu_{\max} = 0.4$.

system throughout the landing run. However, braking systems must also operate when the tire-runway coefficient is very low; the most common cause for low friction coefficients is the presence of water or slush on the runways. For such conditions, a phenomenon commonly called tire hydroplaning or aquaplaning can occur. During complete hydroplaning, the airplane tire is completely supported by the fluid and the wheels may come to a complete stop even though the airplane has an appreciable forward velocity and no braking torque is applied. Much information regarding this phenomenon can be found in the literature. (See, for example, refs. 6, 8, and 9.)

In brief, complete hydroplaning occurs at a velocity which depends primarily on the tire pressure, tread pattern, and fluid depth. For a modern large commercial jet transport having a tire inflation pressure of 150 lbf/in² (103.4 N/cm²), the velocity at which complete hydroplaning begins is approximately 110 knots, and for the tire used in this analysis complete hydroplaning occurs at about 150 knots. As the forward speed drops below the critical speed for complete hydroplaning, the wheel once again contacts the runway surface, and the load supporting the tire is then divided between the fluid and the runway. The distribution of load between the fluid and runway for this partial hydroplaning condition depends primarily on the magnitude of the forward speed.

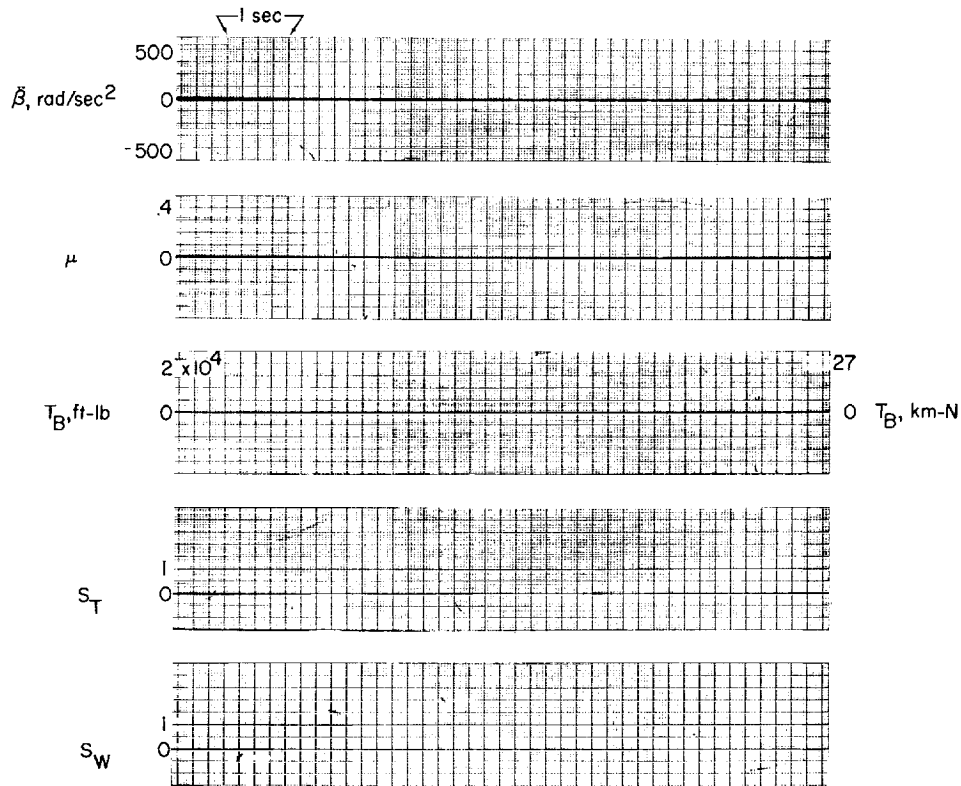


Figure 15.- Concluded.

The manner in which the load is distributed between the fluid and runway determines the amount of retarding force that the braking system can develop; that is, at high forward speeds where a small portion of the load is carried by the runway, the braking forces that can be developed are smaller than those that can be developed at the lower speeds where more of the airplane weight is supported by the runway. Under forward velocity conditions resulting in complete hydroplaning, it is clear that braking systems are completely ineffective and, as a result, during this time the aerodynamic drag developed by the airplane spoilers and wing flaps and reverse engine thrust must be depended on to reduce the speed. Once the speed has been reduced to a level that allows the tires to make contact with the runway, however, the braking system may then become effective in two ways in bringing the airplane to a safe stop: first, by developing a sufficient retarding force throughout the entire distance to stop the airplane in the available runway length with an adequate safety margin; second, by allowing the tires to operate at a minimum slip ratio so that cornering forces can be developed by the rolling tires to maintain directional stability which is lost when the wheels lock up or when the tires operate at high slip ratios. Hydroplaning, as pointed out, depends on velocity; however, other causes of low tire-surface friction coefficients, such as those for icy surfaces, are, in general, quite independent of velocity and exhibit a low coefficient throughout the entire velocity range.

Braking system efficiency.- In order to study the effect of variations in μ_{\max} on the efficiency and performance of braking systems, a series of computer runs were made over a range of μ_{\max} values varying from 0.1 to 0.8. Since the previous results indicated that brake A operating with a control frequency of 5 cycles per second was the most efficient system for $\mu_{\max} = 0.4$ (see fig. 8), this system was used for the first series of runs made over the coefficient-of-friction range. Results showing the efficiency of this braking system are presented in figure 16 by the curve drawn through the circle symbols. For the runs made at μ_{\max} values greater than 0.5, the limiting brake torque of 13,400 foot-pounds (18,167.72 m-N) is less than the product $\mu_{\max} W r_T$; therefore, during these runs the system operated at about the maximum brake torque throughout the entire run with no tire slipping, and the stopping distances were about the same. The apparent increase in efficiency associated with the decrease in μ_{\max} from 0.8 to 0.5 is caused by an increase in the value of minimum runout distance used in computing the efficiency parameter. As μ_{\max} decreases below 0.4, it can be seen that the braking-system efficiency also decreases in this range and reaches a value of less than 50 percent when $\mu_{\max} = 0.1$. This effect is just opposite the effect required to insure safe aircraft operations. To illustrate this point, the efficiency required to stop an airplane over the given coefficient of friction range in 7,000 feet (2,133.60 m) is shown in figure 16 as a dashed line. For $\mu_{\max} = 0.8$, an efficiency of less than 20 percent is required to stop in 7,000 feet (2133.60 m) whereas for $\mu_{\max} = 0.1$, an efficiency of about 90 percent is required. The stopping distance computed for the run (represented by the circle symbol) at

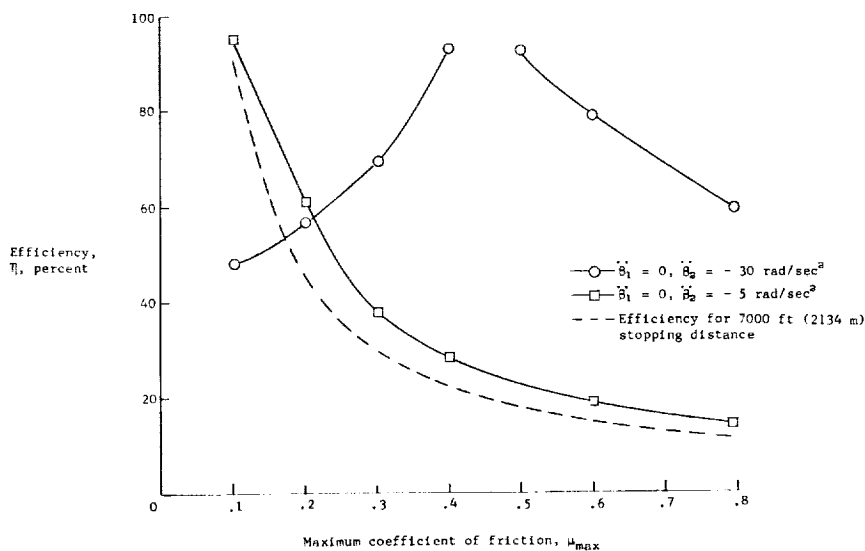


Figure 16.- Effect of varying brake-control signal on the variation of braking-system efficiency with maximum friction coefficient. $t_1 = t_2 = 0.1$ second;

$$\frac{\omega_{n,\beta}}{2\pi} = 5 \text{ cycles/second.}$$

$\mu_{\max} = 0.1$ was around 15,000 feet (4,572 m). This result indicates that a braking system which operated satisfactorily in the presence of relatively high or medium coefficients of friction could operate unsatisfactorily at low coefficients of friction.

In seeking a corrective measure which would involve minimum modifications to the braking system, a series of computer runs were made over the range of friction coefficients with the same brake but changing the value of $\ddot{\beta}_2$, the acceleration at which the control generated a brake-release signal. For these runs $\ddot{\beta}_2$ was made equal to -5 radians per second per second and $\ddot{\beta}_1$ was the same as that for the previous runs, that is, zero. The results of these computer runs are indicated by the square symbols in figure 16. This change resulted in essentially a runout of somewhat less than 7,000 feet (2,133.60 m) for each run over the entire range of μ_{\max} investigated. The computer time histories for both runs appearing in figure 16 that were made at $\mu_{\max} = 0.2$ are shown in figures 17 and 18.

Figure 17 shows the run made with $\ddot{\beta}_2 = -30$ radians per second per second. For the first several thousand feet of runout, braking torque is being cycled very rapidly by the control in the manner discussed earlier. The control is again capable of operating smoothly on the back side of the μ -slip curve for the tire and continues to exercise control until the tire is, for all intents and purposes, in a full skid. For this low μ_{\max} condition, however, the wheel is not able to spin up to full rolling speed and the control continues to operate at this point for the remainder of the run which is very close to $S_T = 1$. This condition, of course, results in much tire skidding. Again, the brake-release signal is probably generated by the low wheel speed control.

In contrast, figure 18 shows that the run made with $\ddot{\beta}_2 = -5$ radians per second per second operates throughout the entire stopping distance with no tire slipping. The fact that for both runs the runout distance or efficiency was practically the same indicates that both operated over the same average value of friction coefficient. The difference being that for the run in which $\ddot{\beta}_2 = -30$ radians per second per second, the braking system operated on the back side of the μ -slip curve for the tire at $\mu \approx \mu_{\text{skid}}$, whereas although the other system operated at about the same average friction value, its operation was on the front side of the μ -slip curve for the tire where no tire skidding occurs.

This optimum type of operation can be explained by noting that the rolling acceleration of the wheel at -5 radians per second per second is equivalent to a linear forward acceleration of -0.18g. Since μ_{\max} was 0.2, it is evident that brake torque was released just before the tire reached the limiting friction value for the runway and although the high-frequency oscillations of $\ddot{\beta}$ are barely perceptible on the record shown in figure 18 because the value is so small, it is evident that the brake torque was controlled at a value that kept the tire rolling without slipping at an apparent coefficient of friction just under μ_{\max} . In other words, having $\ddot{\beta}_2 = -5$ radians per second per second

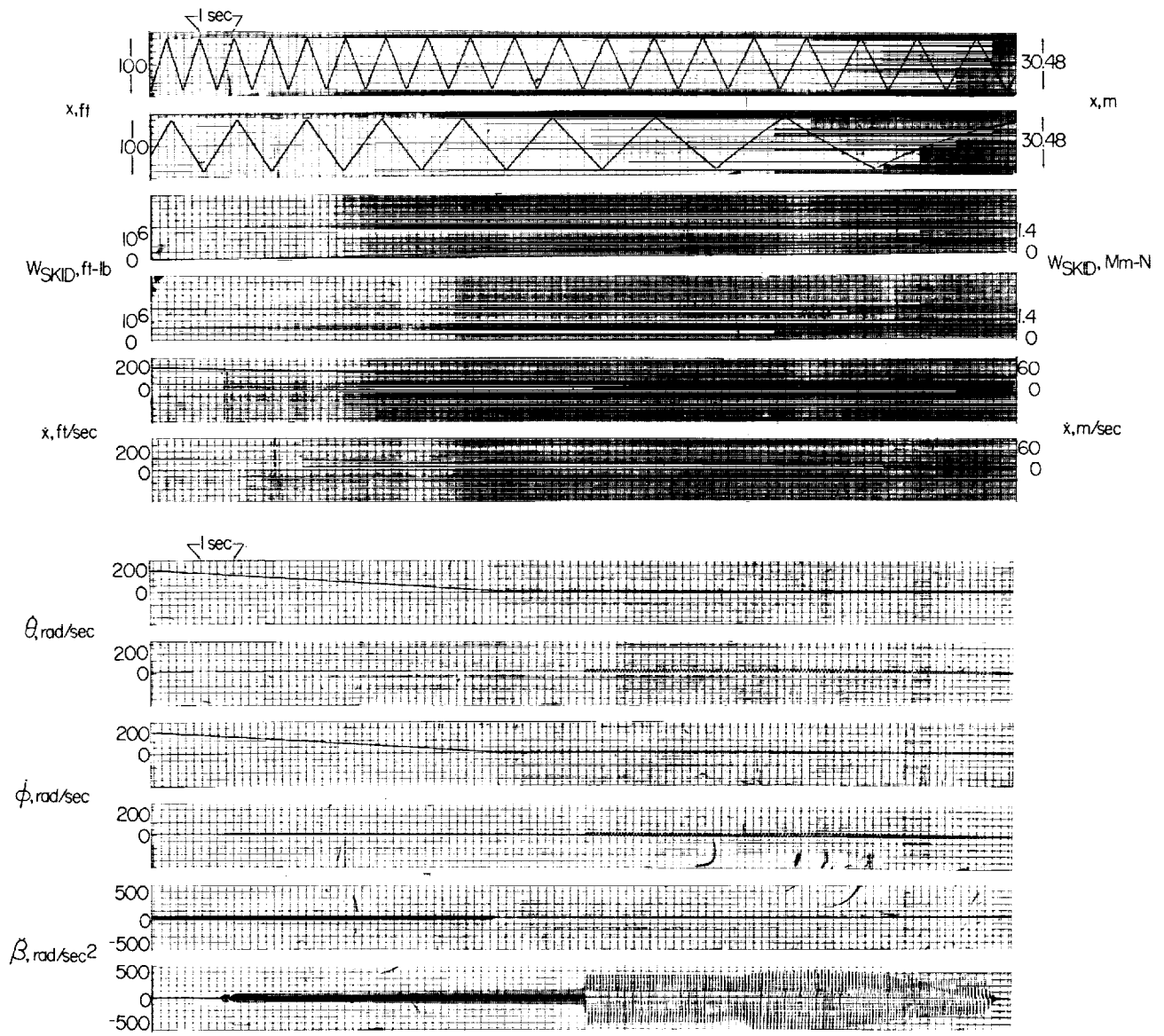


Figure 17.- Analog computer time-history solution. $\ddot{\beta}_1 = 0$; $\ddot{\beta}_2 = -30$ radians/second²;
 $t_1 = t_2 = 0.1$ second; $\frac{\omega_{h,\beta}}{2\pi} = 5$ cycles/second; $\mu_{max} = 0.2$.

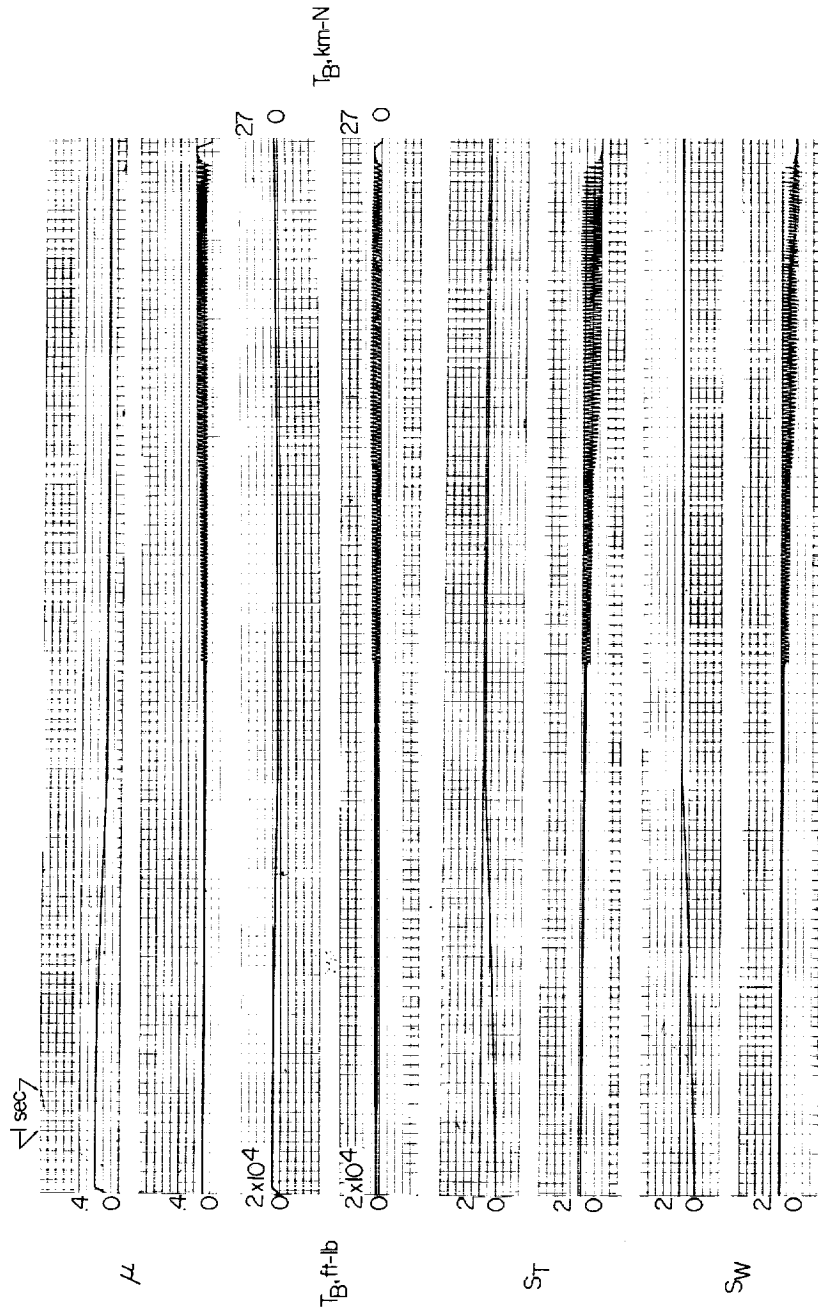


Figure 17.- Concluded.

resulted in a linear deceleration \ddot{x} slightly under that specified by equation (1) for a μ value of 0.2.

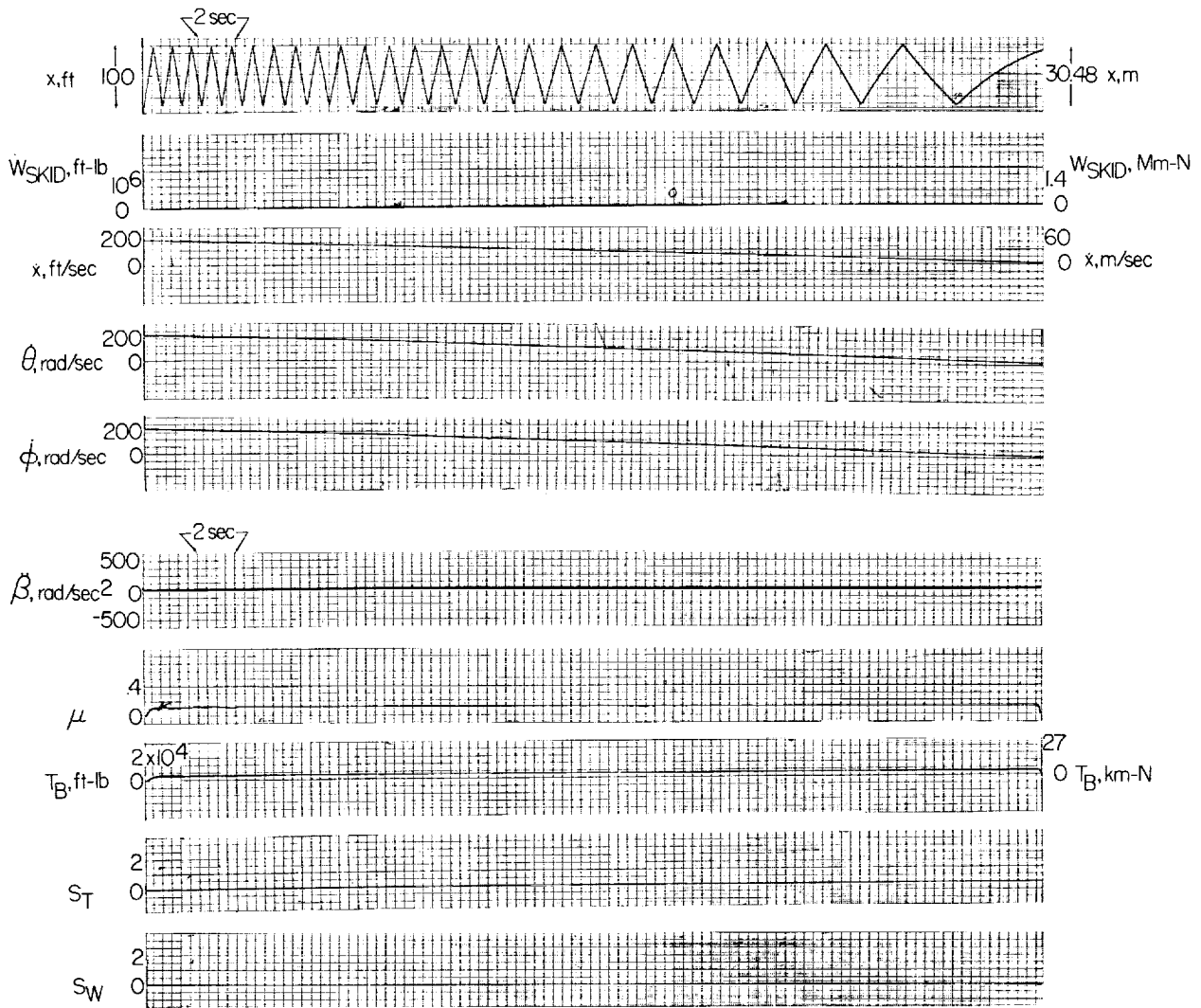


Figure 18.- Analog computer time-history solution. $\ddot{\beta}_1 = 0$; $\ddot{\beta}_2 = -5$ radians/second²;

$$t_1 = t_2 = 0.1 \text{ second}; \frac{\omega_{n,\beta}}{2\pi} = 5 \text{ cycles/second}; \mu_{\max} = 0.2.$$

Figure 19 shows the run made at $\mu_{\max} = 0.1$ with the braking system set so that $\ddot{\beta}_2 = -5$ radians per second per second. Although the tire is slipping throughout most of the run because μ_{\max} is less than 0.18, the increase in slip is very gradual, and as indicated in figure 16, the efficiency for this system is over 90 percent.

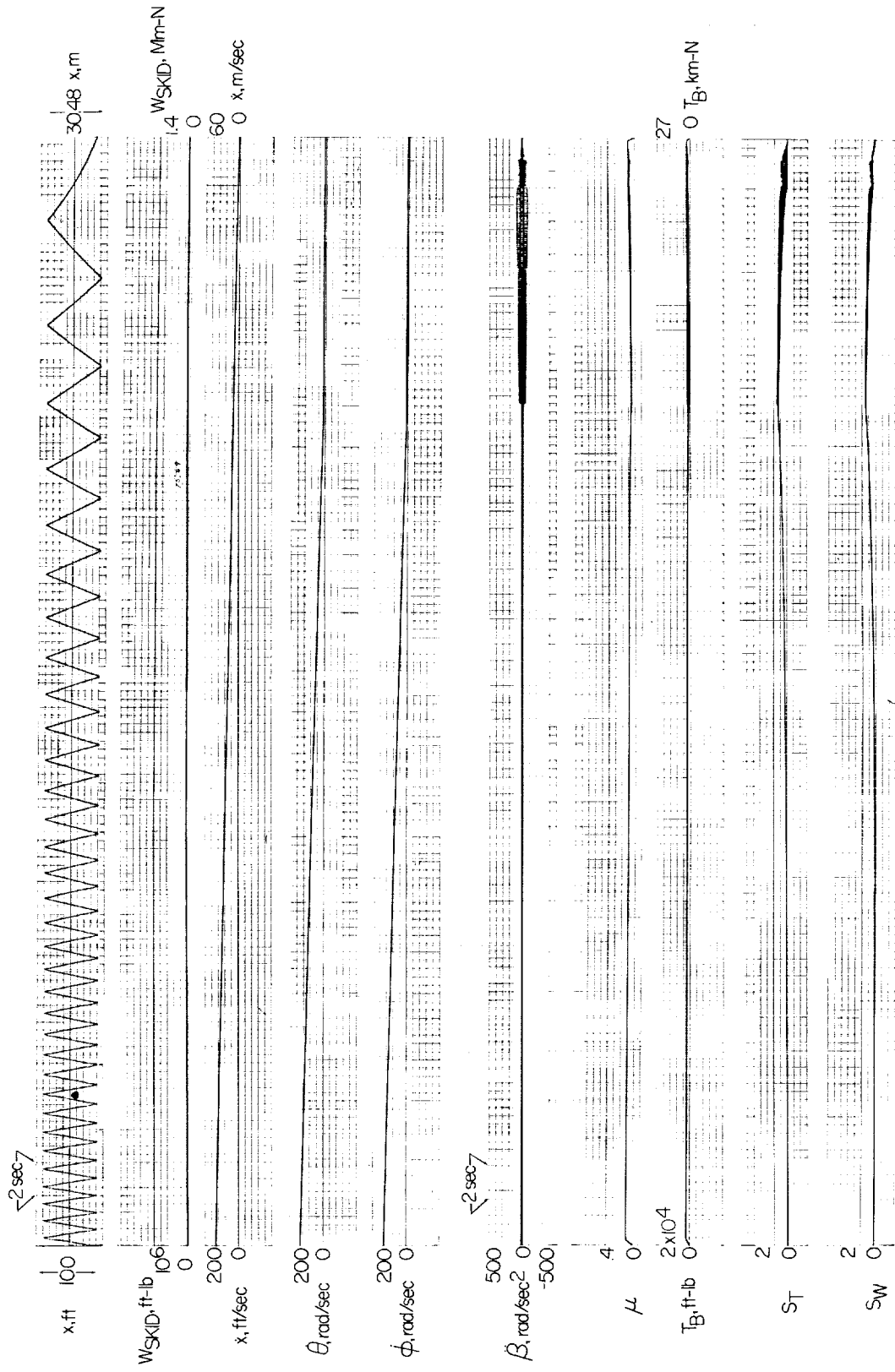


Figure 19.- Analog computer time-history solution. $\ddot{\beta}_1 = 0$; $\ddot{\beta}_2 = -5$ radians/second²; $t_1 = t_2 = 0.1$ second;
 $\frac{\omega_n \beta}{2\pi} = 5$ cycles/second; $\mu_{max} = 0.1$.

Braking-system performance.- The effectiveness of the two braking systems in minimizing tire skidding over the range of friction coefficients is indicated in figure 20. For the braking system in which $\ddot{\beta}_2$ was set at -30 radians per second per second, the percentage of stopping energy contributed by tire skidding rises sharply as the available coefficient of friction decreases, and

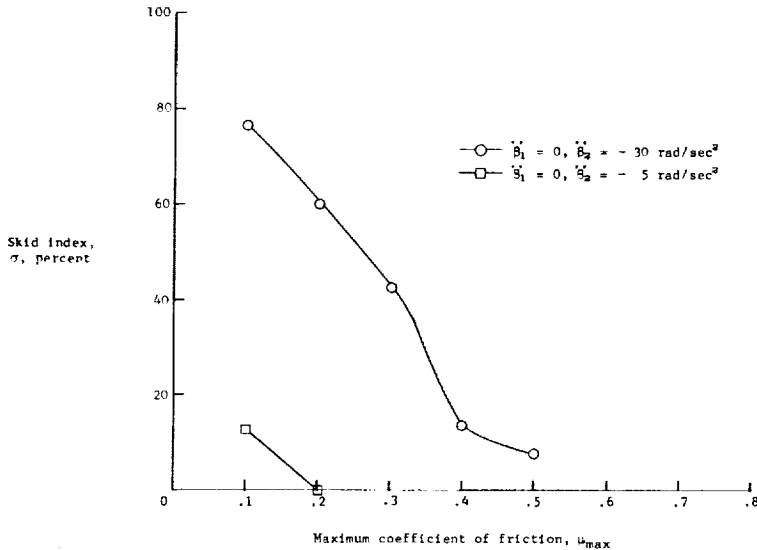


Figure 20.- Effect of varying brake-control signal on the variation of work done by tire in skidding with maximum friction coefficient. $t_1 = t_2 = 0.1$ second;

$$\frac{\omega_{n,\beta}}{2\pi} = 5 \text{ cycles/second.}$$

where $\mu_{max} = 0.1$, almost 80 percent of the stopping energy is contributed by tire skidding. On the other hand, for the system where $\ddot{\beta}_2 = -5$ radians per second per second, tire skidding is evident only for the minimum coefficient of friction of 0.1 and for this case contributes only slightly more than 10 percent of the total stopping energy.

When the performance of a braking system is evaluated with respect to its ability to limit tire skidding, it is important to associate the performance with the magnitude of the available coefficient of friction. Skidding at high coefficients of friction results in excessive tire wear; whereas during skidding at low coefficients of friction, the tire wear is greatly reduced. The importance of maintaining skidding at a minimum during stops at a low coefficient of friction condition is associated with the loss of direction control. During skidding the available cornering force is decreased and becomes zero for a fully locked tire. Needless to say, this condition is a dangerous one, especially if complete locking occurs early in the landing when the forward speeds are greatest. The hazards associated with this condition are discussed in reference 10.

Modulation of brake-release signal.- The results shown in figures 16 and 20 would suggest that a braking system which modulated the value of $\ddot{\beta}_2$ as a function of airplane forward speed could be very effective in achieving safe stops on flooded or slush-covered runways. Such a system could be adjusted so that the deceleration developed by the flaps and spoilers in addition to engine reverse thrust was greater than the initial value of $\ddot{\beta}_2$ that would cause it to release brake torque. As a consequence, no braking would be applied during the early stages of the landing since the wheel deceleration would be greater

than $\ddot{\beta}_2$. Therefore, the full cornering capability of the freely rolling wheels would be available to maintain directional control of the aircraft during this critical stage of the landing runout. Reference 11 indicates that although the aerodynamic drag becomes less as the forward speed decreases, the average deceleration during the early stages of the landing runout attributable to both aerodynamic drag and engine reverse thrust is around 0.2g. As the velocity decreases and the amount of the airplane weight supported by the runway increases, the stopping effort contributed by the brakes could then be augmented by modulating the value of $\ddot{\beta}_2$ to allow the release of brake torque at a larger wheel deceleration.

For the conditions of low friction coefficient which are not largely dependent on velocity, such as ice, the foregoing modulation system could not be used since μ_{\max} would be practically the same for the entire braking stop. It would then be necessary to maintain the original small value of $\ddot{\beta}_2$ for the entire run. The braking process, however, could still be accomplished with high efficiency, as indicated by the curve associated with the square symbols in figure 16. Dispensing with the modulation of $\ddot{\beta}_2$ would, of course, affect the stopping distance.

In this connection, it should be mentioned that low coefficients, which are also largely independent of forward velocity, can be experienced on very smooth damp surfaces. In this case, the low coefficient results from a lubrication process. It was shown in reference 12, however, that by merely making such surfaces rough, very large increases in the coefficient-of-friction values can be realized. It would, therefore, appear that the braking-system problem could be substantially alleviated by insuring that runway surfaces have adequate roughness.

Efficiency.- It should be pointed out that the method which has been used in defining efficiency might be difficult to use in practice. The reason for this difficulty lies in the fact that the numerator of the efficiency term, minimum stopping distance, must be associated with a definite coefficient of friction. Therefore, efficiency, as defined herein, would only take on real meaning when defined as a curve over a specific range of coefficients of friction. The dashed curve in figure 16 is an example of one type of efficiency curve and would be the efficiency curve for a constant stopping distance of 7,000 feet (2,133.60 m).

Variation of μ with S_T for $S_T > 0$.- It was pointed out in the discussion concerning operation of brake A that the slope of the μ -slip curve for the tire in the region where $S_T > 0$ affected the stability of the braking system and therefore had a significant effect on the efficiency and operation of the system. Also, the actual variation of μ with S_T for the region in which $S_T > 0$ could not be described by a unique curve because it depended on a number of variables, some of which varied in a random manner. The slope of the curve used to obtain all the results presented was based on an empirical value determined from experimental data obtained during dry-surface braking tests, and the value of μ_{skid} was about one-third of the μ_{\max} value. It

should be pointed out, however, that the available experimental data appear to indicate that when braking stops are made on surfaces which exhibit low coefficients of friction, the values of μ_{skid} and μ_{max} do not differ in value as much as the dry-surface values. This difference would, of course, affect the slope of the μ -slip curve for the tire. This result would suggest the need for further studies to establish critical variations of μ with S_T compatible with the conditions encountered in practice for use in the design of braking systems.

CONCLUDING REMARKS

A preliminary analog computer study has been made of the operation of an automatically controlled braking system in which the elastic character of the tire and the response time of the brake were taken into account in developing the system equations of motion. These equations were derived in general terms for a simplified single wheel and tire system and then solved on the analog computer for a particular case of a wheel equipped with a 32×8.8 type VII tire. A relation was developed to define the variation of the coefficient of friction with slip ratio and this relation was in agreement with some experimental results. The brake simulation used was torque limited, and the variation of brake torque with time during application and release was assumed to be linear. The solutions indicated that tire elasticity has a very important effect on the operation of the system. For the case of an elastic tire, the wheel motion could differ considerably from the tire motion at various instants of time during the braking process. As a result, during cyclic braking, the variation of the coefficient of friction with wheel slip ratio could have both positive and negative slopes in the region between free rolling and the attainment of maximum friction coefficient. This result is in contrast to current notions since experimental data are normally presented with this slope drawn positive. The results also indicated that the efficiency or stopping capability of an automatic braking system is affected by tire elasticity.

Studies were also made of several brakes having a different variation of torque decay with time. It was found that the braking-system efficiency depended on a complex interaction between the values of tire frequency, brake-response time, and skid-control sensor frequency. The results showed that depending on the combinations of the foregoing factors, the efficiency of the braking systems analyzed varied from better than 90 percent down to 0 percent. It was also found that under certain dynamic conditions, a skid-control sensor with a relatively low response was capable of exercising control of brake torque at a frequency about 18 times its own natural frequency.

Studies were also made of the effect of low tire-ground friction coefficients on the operation of automatic braking systems. The results showed that a braking system which operated satisfactorily in the presence of relatively high or medium coefficients of friction could operate unsatisfactorily at low coefficients of friction. For low friction coefficients, large decreases in both stopping distance and tire skidding could be realized by proper selection of the wheel deceleration value used to generate a brake-release signal. The

results suggested that modulation of this control signal could be very effective in achieving safe stops on water or slush-covered runways.

The results of this preliminary study cannot, however, be considered as a precise description of control-system operation since many factors affecting the operation of a braking system are not presently known. Although the trends indicated herein can be considered valid, further research is needed in areas related to the general mechanical properties of rolling tires, the character of the loads developed by such tires under the influence of brake torque, and the time characteristics of brake-torque variation. A better understanding of these phenomena would result in improved accuracy of the analog simulation and the results would then be more descriptive of those obtained during actual braking stops. The results also suggested the need for further studies to establish critical variations of coefficient of friction with tire slip ratio that would be compatible with conditions encountered in practice.

Langley Research Center,
National Aeronautics and Space Administration,
Langley Station, Hampton, Va., August 16, 1965.

APPENDIX A

DERIVATION OF EQUATIONS OF MOTION

The equations of motion for the mathematical model shown in figure 1 will be obtained using La Grange's equations which are (ref. 13):

$$\frac{d}{dt} \left(\frac{\partial T}{\partial \dot{q}_i} \right) - \frac{\partial T}{\partial q_i} + \frac{\partial V}{\partial q_i} = Q_i \quad (i = x, \theta, \varphi, \beta) \quad (A1)$$

The kinetic energy of the system is

$$T = \frac{1}{2} \frac{W}{g} \dot{x}^2 + \frac{1}{2} I_W \dot{\theta}^2 + \frac{1}{2} I_T \dot{\varphi}^2 + \frac{1}{2} I_\beta \dot{\beta}^2 \quad (A2)$$

The potential energy of the elastic elements of the system are

$$V_T = \int_0^{y_T} k_T y_T dy_T = \frac{k_T y_T^2}{2} \quad (A3)$$

$$V_\beta = \int_0^{y_\beta} k_\beta y_\beta dy_\beta = \frac{k_\beta y_\beta^2}{2} \quad (A4)$$

The generalized forces Q_i are

$$Q_x = -\mu W \quad (A5)$$

$$Q_\theta = T_B + r_W C_\theta (\dot{\varphi} - \dot{\theta}) \quad (A6)$$

$$Q_\varphi = r_T \mu W - r_W C_\varphi (\dot{\varphi} - \dot{\theta}) \quad (A7)$$

$$Q_\beta = -n C_\beta (\dot{\beta} - \dot{\theta}) \quad (A8)$$

The sign of T_B is chosen so that the brake torque always opposes the wheel motion θ .

APPENDIX A

The specific equations of motion when $i = x, \theta, \varphi,$ and β are as follows:

When $i = x$: Substituting equations (A2) and (A5) into equation (A1) gives

$$\ddot{x} = -\mu g \quad (A9)$$

When $i = \theta$: Substituting equations (A2), (A3), (A4), and (A6) into equation (A1) and noting that

$$y_T = r_W(\varphi - \theta)$$

and

$$y_\beta = n(\beta - \theta)$$

gives

$$I_W \ddot{\theta} - k_T r_W^2 (\varphi - \theta) - k_\beta n^2 (\beta - \theta) = T_B + r_W C_\theta (\dot{\varphi} - \dot{\theta})$$

Since the torque produced by the deflection of the control spring is negligible compared with the torque produced by the elastic tire, the term $-k_\beta n^2 (\beta - \theta)$ is dropped and this equation can be written as

$$I_W \ddot{\theta} - k_T r_W^2 (\varphi - \theta) = T_B + r_W C_\theta (\dot{\varphi} - \dot{\theta}) \quad (A10)$$

Also

$$C_{C,\theta} = \frac{2I_W \omega_{n,\theta}}{r_W} \quad (A11)$$

where

$$\omega_{n,\theta} = \sqrt{\frac{k_T r_W^2}{I_W}}$$

Dividing both sides of equation (A10) by equation (A11) and then multiplying both sides by $2\omega_{n,\theta}/r_W$ gives

APPENDIX A

$$\ddot{\theta} - 2\omega_{n,\theta}\xi_{\theta}(\dot{\phi} - \dot{\theta}) - \omega_{n,\theta}^2(\phi - \theta) = \frac{T_B}{I_W} \quad (A12)$$

where

$$\xi_{\theta} = \frac{C_{\theta}}{C_{C,\theta}} \quad (A13)$$

When $i = \phi$: Substituting equations (A2), (A3), and (A7) into equation (A1) gives

$$I_T\ddot{\phi} + k_T r_W^2(\phi - \theta) = r_T \mu W - r_W C_{\phi}(\dot{\phi} - \dot{\theta}) \quad (A14)$$

Also

$$C_{C,\theta} = \frac{2I_T \omega_{n,\phi}}{r_W} \quad (A15)$$

where

$$\omega_{n,\phi} = \sqrt{\frac{k_T r_W^2}{I_T}}$$

Dividing both sides of equation (A14) by equation (A15) and then multiplying both sides by $2\omega_{n,\phi}/r_W$ gives

$$\ddot{\phi} + 2\omega_{n,\phi}\xi_{\phi}(\dot{\phi} - \dot{\theta}) + \omega_{n,\phi}^2(\phi - \theta) = \frac{r_T \mu W}{I_T} \quad (A16)$$

where

$$\xi_{\phi} = \frac{C_{\phi}}{C_{C,\phi}} \quad (A17)$$

By noting that $C_{\phi} = C_{\theta}$, it can be shown that

$$\xi_{\phi} = \xi_{\theta} \sqrt{\frac{I_W}{I_T}} \quad (A18)$$

APPENDIX A

When $i = \beta$: Substituting equations (A2), (A4), and (A8) into equation (A1) gives

$$I_{\beta}\ddot{\beta} + k_{\beta}n^2(\beta - \theta) = -nC_{\beta}(\dot{\beta} - \dot{\theta}) \quad (A19)$$

Also

$$C_{C,\beta} = \frac{2I_{\beta}\omega_{n,\beta}}{n} \quad (A20)$$

where

$$\omega_{n,\beta} = \sqrt{\frac{k_{\beta}n^2}{I_{\beta}}}$$

Dividing both sides of equation (A19) by equation (A20) and then multiplying both sides by $2\omega_{n,\beta}/n$ gives

$$\ddot{\beta} = -2\omega_{n,\beta}\xi_{\beta}(\dot{\beta} - \dot{\theta}) - \omega_{n,\beta}^2(\beta - \theta) \quad (A21)$$

where

$$\xi_{\beta} = \frac{C_{\beta}}{C_{C,\beta}} \quad (A22)$$

Equations (A9), (A12), (A16), and (A21) are the equations of motion of the system and are the same as equations (1), (2), (3), and (4).

APPENDIX B

DERIVATION OF BRAKE-TORQUE EQUATION FOR THE CASE OF A FULLY LOCKED WHEEL

The brake-torque equation for the case of a fully locked wheel is derived in this appendix.

During complete wheel locking

$$\ddot{\theta} = \dot{\theta} = 0 \quad (B1)$$

Also, from appendix A

$$\omega_{n,\theta}^2 = \frac{k_T r_W^2}{I_W} \quad (B2)$$

and

$$\omega_{n,\phi}^2 = \frac{k_T r_T^2}{I_T} \quad (B3)$$

Substituting equations (B1), (B2), and (B3) into equations (A12) and (A16) and then adding the two resulting equations gives

$$I_T \ddot{\phi} + 2\dot{\phi} \left(\omega_{n,\phi} I_T \xi_\phi - \omega_{n,\theta} I_W \xi_\theta \right) - \mu W r_T = T_{B,L} \quad (B4)$$

where $T_{B,L}$ is the symbol for the value of brake torque during the time the wheel is fully locked.

By using the expressions of appendix A for $\omega_{n,\phi}$, $\omega_{n,\theta}$, ξ_ϕ , and ξ_θ , it can be shown that the coefficient of $2\dot{\phi}$ (the expression in parenthesis) in equation (B4) is equal to zero. Therefore, the expression for evaluating brake torque while the wheel is locked is

$$T_{B,L} = I_T \ddot{\phi} - \mu W r_T \quad (B5)$$

Equation (B5) is identical to equation (8).

APPENDIX C

DERIVATION OF THE EQUATION FOR DETERMINING THE WORK DONE BY THE TIRE IN SKIDDING

The work done in skidding is equal to the product of the skidding distance and the ground drag force. Expressed in incremental form:

$$\Delta W_{\text{skid}} = \Delta x_{\text{skid}} \mu W \quad (C1)$$

but

$$\Delta x_{\text{skid}} = \dot{x}_{S_T} \Delta t \quad (C2)$$

Substituting equation (C2) into equation (C1) gives

$$\Delta W_{\text{skid}} = \dot{x}_{S_T} \mu W \Delta t \quad (C3)$$

Dividing both sides of equation (C3) by Δt and letting Δt approach zero as a limit, that is

$$\lim_{\Delta t \rightarrow 0} \frac{\Delta W_{\text{skid}}}{\Delta t} = \frac{dW_{\text{skid}}}{dt} = \dot{x}_{S_T} \mu W$$

Therefore

$$W_{\text{skid}} = W \int_{t=0}^{t=t} \dot{x}_{S_T} \mu \, dt \quad (C4)$$

Equation (C4) is identical to equation (9).

REFERENCES

1. Horne, Walter B.; and Joyner, Upshur T.: Traction of Pneumatic Tires on Wet Runways. Conference on Aircraft Operating Problems, NASA SP-83, 1965, pp. 9-17.
2. Mechtly, E. A.: The International System of Units - Physical Constants and Conversion Factors. NASA SP-7012, 1964.
3. Kummer, H. W.; and Meyer, W. E.: Rubber and Tire Friction. Eng. Res. Bull. B-80, Pennsylvania State Univ., Dec. 1960.
4. Milwitzky, Benjamin; Lindquist, Dean C.; and Potter, Dexter M.: An Experimental Study of Applied Ground Loads in Landing. NACA Rept. 1248, 1955. (Supersedes NACA TN 3246.)
5. Bausback, R. F.; and Steketee, F. D.: Development of a High Efficiency Brake System for Jet Transports. GDC-62-95, Gen. Dyn./Convair, Apr. 5, 1962.
6. Horne, Walter B.; and Leland, Trafford J. W.: Influence of Tire Tread Pattern and Runway Surface Condition on Braking Friction and Rolling Resistance of a Modern Aircraft Tire. NASA TN D-1376, 1962.
7. Smiley, Robert F.; and Horne, Walter B.: Mechanical Properties of Pneumatic Tires With Special Reference to Modern Aircraft Tires. NASA TR R-64, 1960. (Supersedes NACA TN 4110.)
8. Horne, Walter B.; and Dreher, Robert C.: Phenomena of Pneumatic Tire Hydroplaning. NASA TN D-2056, 1963.
9. Sawyer, Richard H.; Batterson, Sidney A.; and Harrin, Eziaslav N.: Tire-to-Surface Friction Especially Under Wet Conditions. NASA MEMO 2-23-59L, 1959.
10. Cobb, Jere B.; and Horne, Walter B.: Performance on Slippery Runways in Crosswinds. J. Air Traffic Control, vol. 6, no. 6, May 1964, pp. 16-20.
11. Nichols, Donald E.: Overall Braking for Jet Transports. Paper No. 60-AV-2, ASME, June 1960.
12. Batterson, Sidney A.: Braking and Landing Tests on Some New Types of Airplane Landing Mats and Membranes. NASA TN D-154, 1959.
13. Timeshenko, S.: Vibration Problems in Engineering. D. Van Nostrand Co., Inc., 1928.